J Mater Sci (2011) 46:4135–4156
DOI 10.1007/s10853-011-5431-x

IIB 2010

Identification of singular interfaces with Δgs and its basis of the O-lattice

W.-Z. Zhang · X.-P. Yang

Received: 27 September 2010 / Accepted: 2 March 2011 / Published online: 22 March 2011

Abstract This article identifies singular interfaces according to singularity in terms of structural defects, including dislocations and ledges. Defect singularities are defined by the elimination of one or more classes of defects, which must be present in the vicinal interfaces. In addition to the three commonly classified structural interfaces, a new type of interface—the CS-coherent interface—is introduced. Singularities in dislocation and ledge structures have been integrated in the study of orientation relationships (OR). The dislocation structures are determined through the O-lattice theory, originally proposed by Bollmann. The basic concepts of the O-lattice and related formulas from the original theory and extended studies are briefly reviewed. According to the theory, singular interfaces exhibiting singularity in the dislocation structures have been identified. An interface that is singular with respect to the interface orientation must be normal to at least one **Δg**, a vector connecting two reciprocal points from different lattices. An interface that is singular also with respect to the OR must obey one or more **Δg** parallelism rules. The selection of proper **Δg**s for different preferred states of interfaces are explained. Identification of singular interfaces with measurable **Δg**s provides a convenient and effective approach to the interpretation of the observed facets and ORs. The ambiguity about the selection of the deformation matrix (**A**) for the O-lattice calculation and the advantage of the O-lattice approach over the approach using the Frank–Bilby equation for the calculation of the interfacial dislocations are clarified. Limitations of the present approach and further study are discussed.

Dedicated to W. Bollmann, the inventor of the O-lattice.

W.-Z. Zhang (✉) · X.-P. Yang
Department of Materials Science and Engineering,
Laboratory of Advanced Materials, Tsinghua University,
Beijing 100084, China
e-mail: zhangwz@tsinghua.edu.cn

Present Address:
X.-P. Yang
Bruker Nano GmbH, Schwarzschildstrasse 12,
12489 Berlin, Germany

Introduction

Morphologies of secondary phases are important features of microstructures of many materials. The embedded crystalline phases generated within a solid crystal via a solid state phase transformation often display fascinating morphologies. Like regular morphologies of various free crystals grown from vapor or liquid, embedded crystals are also often confined by facets of unique crystallographic orientations. These faceted interfaces are the key characteristics for understanding the morphologies.

In principle, the facets either in a free surface of a crystal or in an interface enclosing an embedded crystal in an equilibrium shape can be explained according to their associations with local minima of the surface or interfacial energy, as can be determined by the Wulff construction [1, 2]. The kinetic effect may alter the relative sizes of the facet areas, but it does not change the association between a facet and an energy minimum. Therefore, it is reasonable to explain the observed facets according to local energy minimum. Advanced models and computers have facilitated calculations of surface energy and interfacial energy. However, it demands large computing work to determine the energy variations with surface orientations, which has two degrees (2D) of freedom. The calculation is much more demanding for interfacial energy, since the interfacial

geometry varies in the five-dimensional boundary geometrical phase (5D BGP) space [2]. An effective approach to determine equilibrium shapes of a crystal is to calculate the values of surface energy of a set of facet candidates. These candidates are usually from low index planes of the crystal, such as low index planes of {100}, {110}, {111}, or {112} for a cubic crystal [3–5]. The investigation of morphologies of an embedded crystal will be greatly enhanced if a set of candidates for interface facets are obtainable from a simple way. However, though some interface facets may be parallel to the low index planes of either crystal, other facets are not [6].

Various models have been proposed to interpret the observed interface facets and the corresponding orientation relationship (OR) between the crystals, as summarized in recent reviews [6, 7]. The majority of them are geometric models. The essence of any geometric model is to evaluate the degree of fit in an interface, but different aspects have been emphasized in various geometric criteria, especially those proposed to rationalize the irrational habit planes of precipitates [6, 7]. There is no universal agreement on the energy representation with a specific geometrical parameter. A systematic study of optimal phase boundaries in exsolved alkali feldspars published in 1968 by Bollmann and Nissen [8] represents a pioneering geometric approach. Instead of calculating the interfacial energy, they proposed to use a p parameter ($p = \Sigma|\mathbf{b}_i|^2/\mathrm{d}_i^2$, where $\mathbf{b}_i$ and d_i are the Burgers vector and spacing of the dislocations, with d_i being determined according to a simplified O-lattice. The definition of the O-lattice will be given later). A correlation between a minimum in the energy and in the p value for an optimal interface was implied in this approach, so that the OR between two crystals corresponding to an optimal interface can be identified according to a minimum value of p. Bollmann argued that: "If the problem is to locate an energy minimum without expecting quantitative indications on the energy values, it is sufficient to replace the energy by a function which can be anticipated to vary monotonically with the energy" (p. 227 in [9]). This argument highlights the physical basis that explains why it is possible to identify an optimal interface associated with an energy minimum from a geometric approach.

Instead of using "optimal interfaces", the present article follows the notation given by Sutton and Balluffi [2] and uses the term "singular interfaces" for candidates of interface facets. According to their classification [2], a sharp interface may be singular, vicinal, or general according to whether the associated energy is at, near or far from a local minimum, respectively. Different types of interfaces are also distinct in their structures. The aim of the present study is to distinguish the singular interfaces according to their structures. However, unless an interface is completely free of any defect, it is impossible to conclude whether a defect-containing interface is singular or not only according to its structure. A singular interface must be examined in contrast to any interface in its vicinal orientation. The structure in a singular interface is distinct from that in a vicinal interface by the absence of at least one type of defects, rather than by a low quantity of a type of defects [10]. This distinction is consistent with the structural difference between a singular and a vicinal surface, described in the terrace-ledge-kink model for a surface structure (Ref. to [1]). For example, ledges are absent in a typical singular surface but they are present in any of its vicinal surfaces. In the present study, the singularity rather than a numerical parameter, such as aforementioned p, will be employed as the key character to identify the singular interfaces.

In addition to the ledge defects, which may be present in both surfaces and interfaces, dislocations are the major interfacial defects in most singular and vicinal interfaces. A correct description of the interfacial dislocation structures is essential to identify singular interfaces in terms of dislocation defects. The O-lattice theory [9, 11] developed by Bollmann is the most general geometric theory for quantitative description of a fit/misfit distribution in three dimensions (3D) and the possible dislocation structure in a general interface. Extensions of this theory have been made to enhance the calculation method [12, 13]. The overall theory was considered to be "extremely powerful and capable of describing the interface/facet structure in considerable detail" in a recent review [7]. To recognize Bollmann's significant contribution, the organizers of iib 2010 have arranged a Bollmann Memory Section in iib 2010. In light of this event, it is worth reviewing the main concept of the O-lattice including its extensions and clarifying some misunderstandings about this powerful theory in literature.

This article will start with a general discussion of the possible candidates of singular interfaces. It will be followed by explanations and derivations of the main formulas of the O-lattice theory, which will be applied to determine the dislocation structures and to identify the geometry of singular interfaces. Like the low index reciprocal vectors ($\mathbf{g}$s) used for describing the candidates for singular surfaces, a set of discrete reciprocal vectors, $\Delta\mathbf{g}$s, will be used for describing the candidates for singular interfaces. The link between the singular interfaces and measurable $\Delta\mathbf{g}$s will be elucidated. Ambiguity about the O-lattice calculation and a comparison of the O-lattice theory with the Frank–Bilby equation to calculate the dislocation configurations will be clarified. The limitation of geometrical approaches will be discussed.

Singular interfaces in terms of defects

Two types of interfacial defects considered here are ledges and dislocations. These defects distribute at high energy locations in an interface, with the defect-free regions in lower energy. To specify each type of defects, the structure of the low energy regions needs to be clarified.

Singularity in terms of ledges

Ledge defects in an interface are identified by their step topological feature. The low energy regions between these defects are the terraces in an interface. A common type of terraces in an interface are the same as that in a free surface of a crystal, namely they are parallel to densely packed atomic planes. Such type of ledges may be called atomic ledges. Since these atomic ledges are common in surfaces and interfaces, the candidates for the singular interfaces in terms of these ledge defects can simply be identified according to low index planes in the crystal basis, as for singular surfaces. When the atomic ledges have an overriding effect in the interfacial energy, the resultant singular interface is possibly free of atomic ledges. An interface parallel to a low index plane of one crystal may not be parallel to the low index plane of the other crystal. The OR permitting a ledge-free singular interface should allow two low index planes from different lattices to be parallel to each other. The resultant interface is singular with respect to the change in the interface orientation (IO) and in the OR if the change in the OR destroys the parallelism between the planes. However, if the change in the OR is a rotation in the parallel planes, it does not alter the singularity condition. Thus, the singularity in terms of the ledge defects confines four of five degrees of freedom in the geometry of the singular interface, so that the singular interface is parallel to low index planes from both lattices. The remaining one degree of freedom in the OR may be constrained by minimization of misfit in the interface plane.

The above consideration agrees with the following maximum $\langle d \rangle$ condition indicated by Sutton and Balluffi [2]. They noted that "the lowest possible interfacial energies in a system are associated with the highest possible values of $\langle d \rangle$" (p. 274 in [2]) where $\langle d \rangle$ is the average interplanar spacing of the lattice planes parallel to the interface. In terms of reciprocal vector, a candidate for singular interface according to singularity in the atomic ledge structure is defined by a low index $\mathbf{g}$ from both or either lattice. The interplanar spacing in each lattice is inversely proportional to $|\mathbf{g}|$. Therefore, a singular interface normal to a pair of parallel low index $\mathbf{g}$ of different lattices will be associated with a large $\langle d \rangle$. The maximum $\langle d \rangle$ criterion implies a dominant effect of the ledges on the interfacial energy. This criterion does not have a general applicability, since the atomic ledge energy in metallic materials may be weak [14]. That is why it conflicts the irrational ORs and irrational habit planes frequently observed in metallic systems [6]. To explain the singular interfaces in these cases, one has to consider the other type of defects—dislocations, which is a major concern in this article.

Singularity in terms of dislocations

The dislocation defects for the singularity in an interfacial structure are the misfit dislocations. Good fit is maintained in the low energy regions between these defects. For interfacial misfit to be evaluated, it is important to specify the reference of "fit". A commonly known fit is full coherence, but this type of fit is not general since other kinds of fit also exist in interfaces. Bollmann [11] has named the reference of fit as a preferred state. The preferred state represents a particular structure of fit that tends to exist at individual locals in an interface. For simplicity, the present study assumes a single preferred state in one interface, if not specified otherwise. The borders where the preferred state discontinues define the locations of the misfit dislocations. The Burgers vector of a dislocation is a translation displacement between two lattices. To preserve equivalent structures of a specific preferred state in any adjacent locations, the Burgers vector of the dislocation between the locations must accord with the preferred state. For example, for the fully coherent structure to repeat in the adjacent regions separated by a dislocation, the Burgers vector must come from the lattice translation vectors of the displaced lattice, which can be either lattice. Therefore, identification of the preferred state is essential in a dislocation structure description.

Two types of preferred states have been classified by Bollmann [11]. One is the primary preferred state, which is "*the single crystal state*" (p. 174 in [11]). It describes a one-to-one fit of lattice planes, rows, and points. The corresponding misfit dislocations are the primary dislocations, but usually the term "primary" is omitted. The other type is called secondary preferred state, which is a "*coincidence state*" or "*fractional coincidence state*" (p. 174 in [11]). While the primary preferred state and the associated structure are unique for a given system, the secondary preferred states and corresponding structures for a given system may be various. Bollmann [11] indicated that periodicity is a necessary (but insufficient) condition for a secondary preferred state. In further applications [6] the structures in a plane with dense coincidence site lattice (CSL) points have been taken as the preferred state, rather than a 3D CSL. In terms of structural units, which may be more close to the relaxed interfacial structure than the 2D

CSL pattern, a secondary preferred state may be described with a periodic distribution of small structural units in 2D. These structural units are usually larger than the primitive unit cells in either or both lattices. The interface geometry required to realize a 2D periodic distribution of small structural units in limited types is equivalent to that required to build a 2D CSL of the same periodicity. Therefore, the geometry for a 2D CSL can be used for identifying the geometry for a structure in a secondary preferred state. The secondary dislocations, which are present at locations where the 2D secondary preferred state discontinues, can also be interpreted either as discontinuity of the 2D CSL or as minority structural units in the interface. A well-known example of an interface in a secondary preferred state is a large angle grain boundary when the misorientation is close to some special value so that a CSL in 3D can be constructed with or without a small constraint. Usually when the lattice parameters of the two phases differ significantly, a secondary preferred state also occurs in singular interphase boundaries. The observed faceted interfaces can guide the construction of a constrained CSL for a preferred state in faceted interfaces [15, 16].

When the dislocations have a dominant effect in the interfacial energy, a singular interface is identified according to singularity in terms of the dislocation defects. As expected, an interface exhibiting a continuous preferred state is a singular interface. This interface is free from any dislocations. In contrast to an atomic ledge-free interface, which only requires a proper OR, a dislocation-free singular interface requires special lattice parameters of the crystals separated by the interface, in addition to a proper OR. However, the lattice parameters in a heterophase system and the OR in a homophase system do not usually permit exact fit to be realized in any interface. Therefore, misfit from a preferred state usually exists in an interface and misfit dislocations may be present in the interface. The key to identifying a singular dislocation structure is its singularity character. Namely, a structure is regarded singular fully with respect to the IO if any small deviation in the IO will always lead to the presence of one or more new types of dislocations in the structure. Eliminating one or more types of dislocations is possible in some interfaces that correspond with special ORs. A structure is regarded as singular with respect to the OR, if both forward and backward deviations in the OR will always add one or more new types of dislocations to the structure. The singularity feature stated above will be used to identify singular interfaces in either primary or secondary preferred state.

Remarks about defect terminology and classification

Interfacial structures are often classified according to the degree of coherency. While the classification is convenient for applications, the terminology requires clarification. The concept of coherency mainly applies to interfaces in the primary preferred state. It is reflected in the traditional classification of interfacial structure—coherent, semicoherent, and incoherent interfaces [1, 17]. This classification is inadequate because the interfacial structures in secondary preferred states are missing [17]. To encompass these structures in the classification, we extended the present three types by the addition of a new class of interfaces. The more thorough classification consists of the following four classes of structures:

1. Coherent structure, in which primary preferred state is realized continuously so that "the lattices match exactly at the interface, and 'corresponding' lattice planes and directions are continuous across the interface" as defined by Christian (p. 361 in [17]). A typical example of an interface containing a coherent structure, i.e., a coherent interface, is a coherent twin grain boundary.
2. Semicoherent structure, in which the coherent areas are separated by discrete misfit dislocations. A typical example of a semicoherent interface is a small angle grain boundary [17]. While the term "semi" may imply half coherent, this term is followed here since it has been adopted in relevant books used in worldwide classrooms [1, 2, 17, 18].
3. CS-coherent structure, in which a secondary preferred state is realized either continuously or locally, separated by the secondary misfit dislocations or ledges. "CS" can be considered as abbreviation of "coincidence state", as defined by Bollmann [11] for the secondary preferred state. The term of "CS-coherent" may also be regarded to stand for "coherent at coincidence sites", so that "CS" is in consistent to the abbreviation in broadly used "CSL", which is used for describing the periodicity in the secondary preferred state in a CS-coherent structure. A typical example of a CS-coherent interface is a special large angle grain boundary, corresponding to a small Σ.[1]
4. Incoherent structure, in which neither type of preferred state can hold in any area of meaningful size in the structure. One reason to form incoherent structure is because the misfit from any preferred state is too large. With a tendency to form a preferred state, this structure may still exhibit random coherency. A typical example of this type of incoherent interfaces is a general large angle grain boundary. Another reason is lack of tendency to form any preferred state due to weak interaction across the interface. An example or illustration of this type of incoherent structure can be found in [1] (i.e., p. 304 and 416).

[1] Σ is the ratio of the unit cell volume of the CSL to that of a crystal lattice.

While the aforementioned examples are specific to intergranular boundaries, the classification is also valid for interphase boundaries, which constitutes the central part of the present study. For both intergranular and interphase boundaries, only the structure of coherent interface is distinct from the others, the spectrum of the other three types of interfacial structures is not abruptly discontinuous. The difference between a semicoherent interface and a CS-coherent interface may be indecipherable when the calculated dislocation spacing in a semicoherent interface approaches to a few atomic distances. The distinction between a CS-coherent interface and an incoherent interface becomes vague when the structure units are assorted with many types, thus disrupting the regularity. However, this uncertainty does not affect the present investigation of singular interfaces, since the preferred state in the structure of an observed singular interface in terms of dislocation defects is usually definite.

Which of the four types of interfaces may be singular? The answer depends on what defects are considered for the singularity analysis. Because atomic ledges may be absent in any of the four types of interfaces, a ledge-free singular interface may have any of these structures when the atomic ledges have an overriding effect in the interfacial energy. In other words, an incoherent interface can be a singular interface, identified in terms of singularity in ledge defects. On the other hand, when the dislocation defects have a dominant effect, a coherent interface, free from any dislocation, is certainly a singular interface. A semicoherent and CS-coherent interface may also be a singular interface, if the structure exhibits the singularity property, i.e., an arbitrary deviation in the IO and OR will cause presence of new type(s) of dislocations. An incoherent interface cannot be singular in terms of dislocations, as expected.

The classification based on coherency greatly restricts the geometry in the 3D space for the ORs corresponding to the candidates of singular interfaces in terms of dislocation defects. This is because the misfit in a coherent, semicoherent or CS-coherent interface must be small enough for the regions where the preferred state holds to be sufficiently large. In other words, the misfit must be small for the possible dislocations to be physically perceptible. For a given system, small misfit from a preferred state is permitted by ORs that occupy a minor portion of the OR space. In such a narrow region, proper ORs and discrete IOs for the singular interfaces can be explored according to the dislocation configurations. Beyond these narrow regions in the OR space, in the rest vast regions in the 5D BGP space, incoherent interfaces are obtained. As can be expected, a variation in the OR and IO in these regions does not make a physically significant change in the incoherent structure and energy.

Unlike the ledge-free condition that clearly identifies the candidates of singular interfaces and limits four degrees of freedom in the 5D BGP space, the condition for the singular interfaces dominated by dislocations is not so straightforward. Given a narrow region in the 3D OR space that allows for a preferred state to be realized, what dislocation structure may be present in the interface and what geometry corresponds to a singular interface? These questions can be answered with the following premises: (1) The Burgers vectors are fixed with a selected preferred state; (2) the misfit distribution in an interface is a function of the IO and OR; (3) any misfit from the preferred state in an interface must be accommodated fully by the dislocations. The first and second premises are the results of a spontaneous process driven by a decrease of interfacial energy. The misfit distribution in an interface and the Burgers vectors of the interfacial dislocations depend on the preferred state formed in this process. Once a preferred state that can represent the result of the spontaneous process is properly identified, a set of Burgers vectors can be defined correctly. The third premise is an assumption. Without it, the dislocation structure of an interface would not need to vary with the IO and OR.

Searching for the candidates of singular interfaces according to the singularity in terms of dislocations is the major concern in the rest of the article. With the above premises, the misfit distribution and hence the dislocation structure for a given OR and IO can be calculated with a proper geometry model. Only in special directions can the associated misfit be fully cancelled by one set of dislocations, and only with a particular orientation can an interface contain a minimum set of dislocations. The first step in the calculation is to determine the dislocation structure in a general interface. The O-lattice theory [9, 11] provides a simple but general tool for quantitative descriptions of interfacial dislocations. The main concept and major formulas of this theory will be briefly reviewed below.

Formulation of the O-lattice

Main concept and core equations

The construction of an O-lattice is a conceptual operation by penetrating two rigid lattices into each other, with one point from each lattice at the origin [9, 11]. This operation yields a distribution of good and poor matching zones. For simplicity, let us consider the primary preferred state first. Provided that the misfit strain is small, as required for a semicoherent interface, the good matching zones of a considerable size will form a periodic pattern. Figure 1 is an illustration of a 2D O-lattice formed by the overlapping (100) planes of two identical simple cubic lattices rotated from each other by a small angle. The center of each good

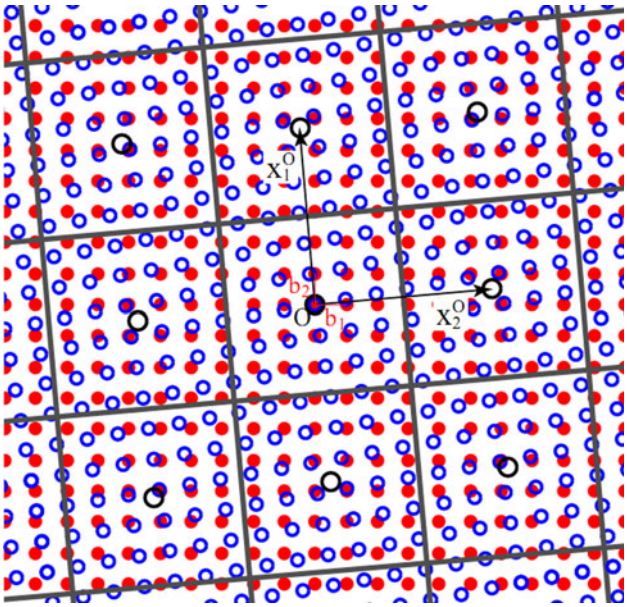

Fig. 1 Illustration of a 2D O-lattice, *dots* and *circles* represent lattice points in different lattices, related by a small angle rotation. Two principal O-lattice vectors, $\mathbf{x}_1^O$ and $\mathbf{x}_2^O$ and their corresponding Burgers vectors b_1 and b_2 defined in the lattice with (*red*) *dots* are marked

matching zone defines an O-element, and the periodic distribution of the O-elements form the O-lattice.[2] In the direction of the rotation axis, normal to the plane of the figure, the 2D O-lattice pattern in Fig. 1 can be obtained in each layer of the lattice plane. From this, one obtains a line lattice in 3D, the O-line lattice with the lines parallel to the rotation axis, as illustrated in Fig. 2. The poor matching regions around each O-line element form an O-cell structure. The individual O-cells contact at the O-cell walls, which define the locations in the poorest match. The structure of the O-lattice depends on the structures of the crystal lattices and the OR. In general, the O-elements in 3D may take a shape of a point, a line, or a plane.

A selected interface is then cut through the O-lattice. The traces of the O-cell walls in the interface, as the intersections of the interface with the O-cell walls, are the poorest matching regions in the interface. These O-cell wall traces have been considered to represent the possible locations of dislocations [9]. Three interfaces and the dislocation structures in the interfaces are illustrated in Fig. 2. In the twist grain boundary normal to the rotation axis, there is a square net consisting of two sets of screw dislocations. In the symmetric tilt grain boundary containing

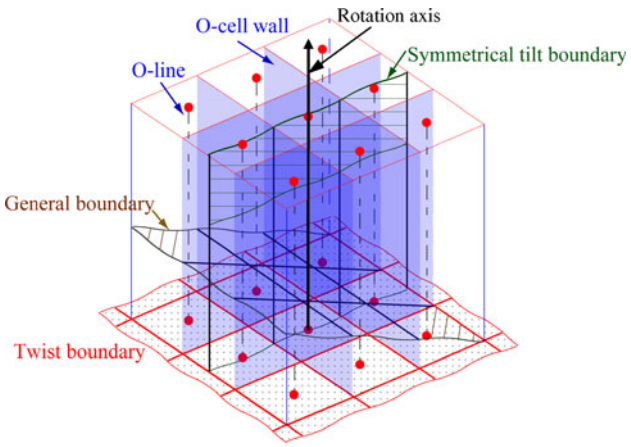

Fig. 2 Illustration of an O-line lattice, O-cell walls, and possible dislocation structure in a twist, a symmetric tilt, and a general grain boundary

the rotation axis, there is a set of parallel dislocations. In the inclined boundary, there are two sets of dislocations, including one set of mixed dislocations. While Fig. 2 clearly illustrates the relationship between the O-lattice/O-cell structures and the structures of interfacial dislocations, these cases are not general and may be misleading. Only when an O-element or an intersected O-element is found in each area separated by an O-cell wall trace, to serve as the center of the coherent zone, can the O-cell wall trace represent dislocation between the coherent zones. Otherwise, it is inappropriate to treat an O-cell wall trace as the position of a dislocation. All three selected interfaces in Fig. 2 satisfy the above requirement. However, an interface in an arbitrary orientation may not satisfy the above requirement, especially when the O-lattice is a point lattice. As explained later, the dislocations structure in any singular interface can meet the above requirement.

The O-lattice can be calculated according to a misfit analysis [9]. In a selected orthonormal coordinate basis, we may express the two lattices (specified as lattices α and β, respectively) according to a given OR. Any position in lattice α can be defined with a vector $\mathbf{x}_\alpha$, and the same holds for lattice β with $\mathbf{x}_\beta$. In the following derivation, we again assume an interface in the primary preferred state. Let us consider the O-cell centered at the origin. In this center O-cell, a group of points in lattice α will become coherent with a group of points in lattice β in a one-to-one base in a semicoherent interface. Upon relaxation, each coherent pair spontaneously forms from the nearest neighbor points in the O-cell. Therefore, the displacement due to the misfit strain in the coherent zone is established between pairs of points in the nearest neighbor. Let a pair of such points be specified by two vectors, $\mathbf{x}_{\beta o}$ and $\mathbf{x}_{\alpha o}$ (column vectors). The misfit displacement between the points is defined by

[2] The O-lattice has been defined as a lattice of origins according to Bollmann [9, 11]. In this sense, the "O" is the abbreviation of origin. However, it can also be considered as the abbreviation of "zero" [11], as used in early publications by Bollmann, e.g. [9]. In this article, the letter O is adopted, since it is well-accepted pronunciation in the community with the O-lattice applications.

$$\Delta \mathbf{x}_{\mathrm{m}} = \mathbf{x}_{\beta \mathrm{o}} - \mathbf{x}_{\alpha \mathrm{o}}. \quad (1)$$

It is convenient to relate such a pair of $\mathbf{x}_{\beta \mathrm{o}}$ and $\mathbf{x}_{\alpha \mathrm{o}}$ with a transformation or a deformation matrix, so that

$$\mathbf{x}_{\beta \mathrm{o}} = \mathbf{A}\mathbf{x}_{\alpha \mathrm{o}} \quad (2)$$

For the example in Fig. 1, **A** is simply a rotation matrix with a small rotation angle. In the O-lattice theory [9], the displacement is associated with a point in lattice β. It will be called the identification lattice for convenience. Based on Eqs. 1 and 2, the misfit associated with $\mathbf{x}_{\beta \mathrm{o}}$ can be determined from

$$\Delta \mathbf{x}_{\mathrm{m}} = (\mathbf{I} - \mathbf{A}^{-1})\mathbf{x}_{\beta \mathrm{o}} = \mathbf{T}\mathbf{x}_{\beta \mathrm{o}}. \quad (3)$$

where **I** is a unit matrix, and $\mathbf{T} = \mathbf{I} - \mathbf{A}^{-1}$, describing the displacement field.

Next we determine the misfit displacement associated with a general point, $\mathbf{x}_{\beta}$, in the identification lattice. One can calculate the displacement associated this point due to the displacement field by

$$\Delta \mathbf{x} = \mathbf{x}_{\beta} - \mathbf{x}_{\alpha} = \mathbf{T}\mathbf{x}_{\beta}. \quad (4)$$

When the point defined by $\mathbf{x}_{\beta}$ is out of the center O-cell, the above $\Delta \mathbf{x}$ does not define the misfit associated with $\mathbf{x}_{\beta}$. This is illustrated in Fig. 3, where $\Delta \mathbf{x}$ is larger than a Burgers vector. The misfit displacement associated with the point defined by $\mathbf{x}_{\beta}$ is evaluated between it and the point in lattice α in its nearest neighbor. This particular point in α can be translated from $\mathbf{x}_{\alpha}$ by a lattice translation vector in α. In the example in Fig. 3, the lattice translation vector is $\mathbf{b}_2$, as indicated in the figure. In general, a translation vector can be written as $\Sigma \mathrm{k}_j \mathbf{b}^{\mathrm{L}}_{\alpha j}$, where $\mathbf{b}^{\mathrm{L}}_{\alpha j}$ is a Burgers vector, k_{j} is an integer, and j denotes different Burgers vectors and corresponding integer coefficients. Therefore, a misfit displacement associated with a general $\mathbf{x}_{\beta}$ can be expressed by

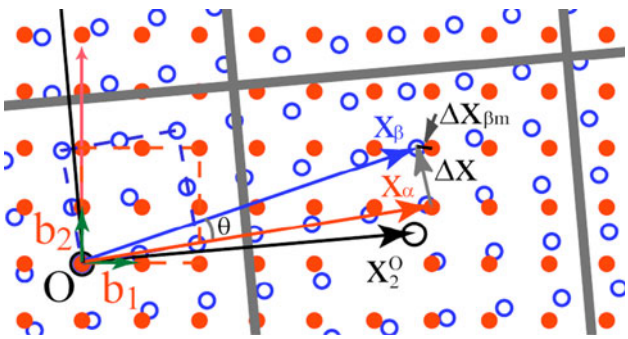

Fig. 3 Comparison of displacement ($\Delta \mathbf{x} = \mathbf{x}_{\beta} - \mathbf{x}_{\alpha}$) and misfit displacement ($\Delta \mathbf{x}_{\beta \mathrm{m}} = \mathbf{x}_{\beta} - \mathbf{x}_{\alpha} - \mathbf{b}_2$) associated with a point defined by $\mathbf{x}_{\beta}$. *Dots* (*red*) and *circles* (*blue*) represent points in lattice α and β, respectively

$$\Delta \mathbf{x}_{\beta \mathrm{m}} = \mathbf{x}_{\beta} - (\mathbf{x}_{\alpha} + \Sigma \mathrm{k}_i \mathbf{b}^{\mathrm{L}}_{\alpha i}) = \mathbf{T}\mathbf{x}_{\beta} - \Sigma \mathrm{k}_i \mathbf{b}^{\mathrm{L}}_{\alpha i}, \quad (5)$$

upon the condition that $|\Delta \mathbf{x}_{\beta \mathrm{m}}| \leq |\Delta \mathbf{x}_{\beta \mathrm{m}} \pm \mathbf{b}^{\mathrm{L}}_{\alpha \mathrm{J}}|$. From Eq. 5 one notices that no misfit is associated with $\mathbf{x}_{\beta}$ if

$$\mathbf{T}\mathbf{x}_{\beta} = \Sigma \mathrm{k}_i \mathbf{b}^{\mathrm{L}}_{\alpha i}. \quad (6)$$

Equation 6 is a general equation for all possible O-elements, as defined by the positions of no misfit. When $\mathrm{Rank}(\mathbf{T}) = 3$, there is a one-to-one correspondence between the points in lattice α (called reference lattice) and the O-point. One can construct the O-lattice using three non-coplanar principal O-lattice vectors, $\mathbf{x}^{\mathrm{O}}_1$, solved from [9]

$$\mathbf{T}\mathbf{x}^{\mathrm{O}}_i = \mathbf{b}^{\mathrm{L}}_{\alpha i}. \quad (7)$$

The above is the core O-lattice equation derived by Bollmann [9]. It states that the relative displacement associated with a point of lattice β at $\mathbf{x}^{\mathrm{O}}_i$ is a Burgers vector in lattice α, $\mathbf{b}^{\mathrm{L}}_{\alpha i}$. When the $\mathrm{Rank}(\mathbf{T}) < 3$, periodic O-elements are usually not solvable for a heterophase system. However, it is often possible to define a single set of O-lines for $\mathrm{Rank}(\mathbf{T}) = 2$, and for one layer of the O-plane for $\mathrm{Rank}(\mathbf{T}) = 1$. This solution of O-lines or O-plane is sufficient to identify one singular interface of the system.

Usually, an O-element is not found at the position of a lattice point, as seen in Figs. 1 and 3. However, the misfit displacement always increases linearly from each O-element. Thus, the misfit associated with the lattice points in the vicinity of an O-element is always small. Provided that the size of the O-cells is considerably larger than the atomic spacing, each O-element can represent a true center of a coherent region in a relaxed structure. If $\mathbf{x}^{\mathrm{O}}_i$ happens to end at a lattice point in β, then $\mathbf{x}^{\mathrm{O}}_i$ defines a coincidence site, where two lattice points exactly match. Therefore, given a proper OR and lattice parameters, the CSL can be calculated as a sublattice of the O-lattice for the primary preferred state, even though the primary preferred state may be imperceptible when the O-cell is too small.

Selection of **A**

Consensus has not been reached yet about whether the misfit distribution defined by an O-lattice can be used to calculate a dislocation structure. A common criticism to a dislocation model, including the O-lattice theory [9] and with the Frank–Bilby equation [19, 20], points out that "there is an infinite number of dislocation descriptions of a particular interface" (p. 93 in [2]). This ambiguity stems from the symmetry operations of either lattice. This operation does not change the relative positions of the atoms, but was speculated to make changes in matrix **A**, and hence influencing the calculated O-lattice and dislocations

structures. Therefore, in order to describe a true dislocation structure, a careful selection of a proper and unique **A** is critical to the model. Bollmann has provided the following criterion for **A**: "The nearest neighbors in both lattices are related by that the transformation **A** selected from various possibilities for which the determinant $|\mathbf{I} - \mathbf{A}^{-1}|$ acquires the smallest absolute value" (p. 165 in [9]). Though the above statement may hold true for some cases, the nearest neighbors may not always be related according to minimization of $|\mathbf{I} - \mathbf{A}^{-1}|$. A widely used example to show the drawbacks of this criterion [2, 17] is that a rational symmetrical tilt small angle grain boundary may be described as a coherent twin boundary, corresponding to zero value of $|\mathbf{I} - \mathbf{A}^{-1}|$. However, a more physically realistic description is a semicoherent boundary containing an array of edge dislocations (as seen from Fig. 2). In this particular example, the nearest neighbors are not related by an **A** selected from the twin relations for $|\mathbf{I} - \mathbf{A}^{-1}| = 0$, but by a small angle rotation as can be seen from Figs. 1 and 3.

The above ambiguity in selecting **A** can be eliminated by clarifying the preferred state. It is crucial that the misfit is evaluated according to the smallest deviation from the unique preferred state. For an interface in the primary preferred state, it is straightforward to identify potential coherent point pairs by forcing local coherency, as seen in the standard dislocation model of a small angle grain boundary in a textbook (e.g., [18]). In the center O-cell, such a relationship between pairs of points indexed in their own lattices can be called lattice correspondence, as used in the phenomenological theory of martensite crystallography (PTMC) [21]. According to the positions in a common coordinate basis for a set of three related non-coplanar vectors $\mathbf{x}_{\beta oi}$ and $\mathbf{x}_{\alpha oi}$ ($i = 1, 2, 3$), matrix **A** is uniquely determined by $\mathbf{A} = \mathbf{X}_{\alpha o}\mathbf{X}_{\beta o}^{-1}$, where $\mathbf{X}_{\alpha o} = [\mathbf{x}_{\alpha o1}, \mathbf{x}_{\alpha o2}, \mathbf{x}_{\alpha o3}]$, and $\mathbf{X}_{\beta o} = [\mathbf{x}_{\beta o1}, \mathbf{x}_{\beta o2}, \mathbf{x}_{\beta o3}]$(The vectors are 1×3 column vectors in the matrixes). The rotation matrix **A** determined from the unique corresponding vectors $\mathbf{x}_{\beta oi}$ and $\mathbf{x}_{\alpha oi}$, expressed in any common coordinate basis can lead to a correct periodicity in misfit variation, as shown in Fig. 1. For the case of a small angle grain boundary, one may simply choose $[100]_\alpha$, $[010]_\alpha$, $[001]_\alpha$ for $\mathbf{x}_{\alpha o1}$, $\mathbf{x}_{\alpha o2}$, $\mathbf{x}_{\alpha o3}$, respectively. If the basis of one lattice is rotated with respect to the other by a small angle, then the corresponding $\mathbf{x}_{\beta o1}$, $\mathbf{x}_{\beta o2}$, $\mathbf{x}_{\beta o3}$ are $[100]_\beta$, $[010]_\beta$, $[001]_\beta$. When a symmetry operation is applied to either lattice, say β, the axes close to $[100]_\alpha$, $[010]_\alpha$, $[001]_\alpha$ become $[010]_\beta$, $[-100]_\beta$, $[001]_\beta$ for example. This operation obviously increases the angle between the two lattice bases. According to the nearest neighbor principle, a new lattice correspondence will be taken, but the positions of $\mathbf{x}_{\beta oi}$ in the selected common coordinate basis remain the same. Therefore, a symmetry operation of either lattice only changes the variant of OR, but the matrix **A** is unchanged. A step-by-step calculation of the O-lattice for an fcc/bcc interface has been provided by Bollmann [22]. In this application, the well-known Bain lattice correspondence, commonly used in the PTMC [21], was assumed at the beginning of this calculation. With this lattice correspondence, the matrix **A** for the given OR is uniquely determined.

The lattice correspondence according to the possibly forced coherence in the center O-cell is consistent with the nearest neighbor principle summarized by Bollmann, who states that "In the proximity of the origin, the transformation **A** must relate the nearest neighbors in the two lattices" (p. 184 in [9]) (The criterion of the smallest $|\mathbf{I} - \mathbf{A}^{-1}|$ was also suggested in his summary, but this part is abandoned to avoid a confusion). This principle ensures that the displacement associated with $\mathbf{x}_{\beta o}$, as determined from Eq. 3, is the misfit displacement between $\mathbf{x}_{\beta o}$ and its nearest $\mathbf{x}_{\alpha o}$.

The nearest neighbor principle is also applicable to a secondary preferred state. Usually, selecting a correct **A** for a CS-coherent interface is not as straightforward as for a semicoherent interface. In the primary preferred state, a group of continuously distributed lattice points within an O-cell can become coherent in a semicoherent interface. In contrast, in a secondary preferred state, the points that can become coherent with their nearest neighbors across the interface may be separated by non-coherent points within an O-cell. The lattice correspondence between these fractional coherent points (i.e., coincident sites) is essential for determination of **A**. One needs to draw a reference of the secondary preferred state, in which either lattice is deformed so that the points related by the lattice correspondence can form a constrained CSL. According to this correspondence, three small none-coplanar vectors from each lattice can be selected to calculate the **A** matrix in the same way as that for the primary preferred state. An example of the selection of a lattice correspondence for a secondary preferred state and a calculation of secondary dislocations can be found in a study of the habit planes between cementite and austenite [15].

Determination of dislocation structures

Calculation of the O-cell walls

In general, the O-lattice structure alone is insufficient in specifying the O-cell structure. The possible dislocation structure is derived from the geometry of the O-cell. According to Bollmann [9], the position of an O-cell wall is confined by the equal misfit condition. This states that the misfit displacement associated with any point, $\mathbf{x}_{c\beta}$, in an O-cell wall of the center O-cell should have identical magnitudes with respect to the origin and the next O-element separated by the wall. This condition can be expressed as [23]

$$\left|\mathbf{T}\mathbf{x}_{c\beta}\right| = \left|\mathbf{T}(\mathbf{x}_{c\beta} - \mathbf{x}_i^{O})\right| = \left|\mathbf{T}\mathbf{x}_{c\beta} - \mathbf{b}_{\alpha i}^{L}\right|. \tag{8a}$$

It can be transformed to the following form

$$\mathbf{b}_{\alpha i}^{L\prime}/|\mathbf{b}_{\alpha i}^{L}|\mathbf{T}\mathbf{x}_{c\beta} = |\mathbf{b}_{\alpha i}^{L}|/2, \tag{8b}$$

where prime "′"denotes a transposition operation to a vector (or to a matrix referred to later). Equation 8a is equivalent to but simpler than the general equation for the O-cell wall in Bollmann's book [9]. One solution of $\mathbf{x}_{c\beta} = \mathbf{x}_i^{O}/2$ was provided in the book, but this was insufficient in specifying the O-cell wall.

It is convenient to define a set of periodically distributed O-cell walls with a reciprocal vector, $\mathbf{c}_{\beta i}^{O}$, such that the O-cell walls are normal to $\mathbf{c}_{\beta i}^{O}$ and their spacing is given by $1/|\mathbf{c}_{\beta i}^{O}|$. Since the O-cell walls are symmetrically placed with respect to the origin, the projection of a general point $\mathbf{x}_{c\beta}$ in the center O-cell onto such a reciprocal vector is $1/(2|\mathbf{c}_{\beta i}^{O}|)$, namely, $\mathbf{c}_{\beta i}^{O\prime}/|\mathbf{c}_{\beta i}^{O}|\mathbf{x}_{c\beta} = 1/(2|\mathbf{c}_{\beta i}^{O}|)$, or

$$\mathbf{c}_{\beta i}^{O\prime}\mathbf{x}_{c\beta} = 1/2. \tag{9}$$

Comparing Eq. 8b and 9, one obtains [13, 23]:

$$\mathbf{c}_{\beta i}^{O} = \mathbf{T}'\mathbf{b}_{\alpha i}^{*}, \tag{10a}$$

where

$$\mathbf{b}_{\alpha i}^{*} = \mathbf{b}_{\alpha i}^{L}/|\mathbf{b}_{\alpha i}^{L}|^2, \tag{10b}$$

is a reciprocal Burger vector in lattice α. It represents a set of parallel faces (normal to $\mathbf{b}_{\alpha i}^{L}$) of the Wigner–Seitz cells in lattice α. Therefore, each set of O-cell walls corresponds to a $\mathbf{b}_{\alpha i}^{L}$, which is the Burgers vector of the dislocations to be determined from the geometry of the O-cell walls. This $\mathbf{b}_{\alpha i}^{*}$ is different from the reciprocal Burgers vector defined by Hirth and Lothe [24]. In their definition, a reciprocal Burgers vector for a set of dislocations is actually a reciprocal vector for a set of (low index) lattice planes that contain two other Burgers vectors (from the three selected non-coplanar $\mathbf{b}_{\alpha i}^{L}$) that are not the Burgers vector of the dislocation set. These reciprocal vectors are represented by $\mathbf{g}_p$ in the present article to follow the convention of electron microscopy terminology in experimental study, as will be used later.

It can be shown (Ref. Eq. 12) that Eq. 10a is an O-lattice transformation in reciprocal space, so that the O-cell is transformed from the Wigner–Seitz cell of lattice α [13]. When Rank($\mathbf{T}$) = 3, the number of O-cell faces is equal to the number of faces of the Wigner–Seitz cells in lattice α, which usually has the same number as the number of attainable $\mathbf{b}_{\alpha i}^{L}$. The above result agrees with Bollmann's interpretation of the O-cells [9], which has stimulated the derivation of the expression in Eq. 10a. As seen from the difference in Eqs. 7 and 10a, $\mathbf{c}_{\beta i}^{O}$ is not generally parallel to $\mathbf{x}_i^{O}$, so that the O-cells are not the Wigner–Seitz cells of the O-lattice. Exceptions occur when the misfit strain field is isotropic in appropriate dimensions, such as an isotropic deformation for an O-point lattice or a rotation in a close packed plane for an O-line lattice [23]. Then, both O-lattice and O-cell will inherit the symmetry of either lattice, and hence the shape of the O-cell is the same as the shape of the Wigner–Seitz cell of either lattice. This explains why the O-cells are the Wigner–Seitz cells of the O-lattice in many O-lattice illustrations with simple examples of the above cases, such as in Fig. 1. To avoid misleading by these special examples, it is emphasized here that the O-cells are generally *not* the Wigner–Seitz cells of the O-lattice. It is worth noting that the walls of a Wigner–Seitz cell in lattice α and its transformed O-cell are usually not continuous in space. They stop at intersections with two other walls, such as where three walls meet. The O-cell structure in Fig. 2 only consists of two sets of walls, so those walls can extend endlessly.

The O-cell structure defined by Eq. 10 is based on evaluation of displacement associated with points in lattice β as the identification lattice. Usually, if an identification lattice changes to lattice α, the O-cell geometry will differ slightly, as indicated by Bollmann [9]. Only for an isotropic transformation, will different identification lattices lead to an identical O-cell structure [23]. In this case, one can calculate $\mathbf{c}_{\beta i}^{O}$ from the vector form of $\mathbf{c}_{\beta i}^{O} = \Delta\mathbf{b}_i^{*} = \mathbf{b}_{\alpha i}^{*} - \mathbf{b}_{\beta i}^{*}$, where $\mathbf{b}_{\beta i}^{*}$ is a reciprocal Burgers vector in lattice β. In this special case, one finds that $\mathbf{b}_{\beta i}^{*} = (\mathbf{A}^{-1})'\mathbf{b}_{\alpha i}^{*}$. A recent investigation indicated that the discrepancy in the dislocation structure due to different selections of the identification lattice only occurs if the structure dislocations comprise of more than two sets of dislocations [23]. This is because dislocations in a one-set structure run along the unique invariant line in the interface, whereas those in a two-set structure run along $\mathbf{x}_i^{O}$, which is independent of the selection of an identification lattice. One attempt involved using the average of O-cell structures from both identification lattices [23]. However, the difference between the observed dislocations in a real boundary and the calculated configuration is likely more prominent in a structure of three-set dislocations than that in a structure of two- or one-set dislocations. For a three-set structure, the deviation of the calculated configuration from the observed result is possibly larger than the discrepancy due to different identification lattices. It would thus be impractical to refine the O-cell wall results when there are three sets of dislocations. Therefore, lattice β will be used in the following calculation of the dislocation structures.

Calculation of interfacial dislocations

When periodic dislocations are observed in a semicoherent interface without long-range strain, there is no reason for the dislocation periodicity to disagree with the misfit distribution in the interface, provided that the preferred state of "fit" in the dislocation-free regions is correctly defined. A calculated dislocation structure based on the O-lattice and the O-cells should closely resemble the true dislocation configuration, since the structure of the O-lattice and the O-cells represent the good and poor matching regions in space, respectively.

According to Bollmann [9], the intersections of an interface with the O-cell walls, or the O-cell wall traces in an interface, represent the dislocations. It must be emphasized that for an O-cell wall trace to represent a dislocation, each of the two areas separated by this trace should contain an O-element. This condition (short for "trace condition" for convenient) ensures equivalent relaxation in both sides of the trace, with the O-elements serving as the centers of the coherent regions. Therefore, the dislocation position can be approximately represented by the O-cell wall trace bisecting a pair of O-elements. To calculate the spacing of a set of periodic dislocation, we assume that the interface satisfy the above condition. Specifically, provided that Burgers vector of the dislocations is $\mathbf{b}^{\mathrm{L}}_{\alpha i}$, the interface must contain the corresponding $\mathbf{x}^{\mathrm{O}}_{i}$ connecting a row of periodic O-elements. Thus, there is always an O-element between adjacent traces of O-cell walls $\mathbf{c}^{\mathrm{O}}_{\beta i}$ corresponding to the same $\mathbf{b}^{\mathrm{L}}_{\alpha i}$. Given the unit normal ($\mathbf{n}$) of such an interface, the direction of the dislocations is defined by the following vector [13]:

$$\boldsymbol{\xi}_{\mathrm{i}} = \mathbf{c}^{\mathrm{O}}_{\beta \mathrm{i}} \times \mathbf{n}, \tag{11a}$$

and the dislocation spacing is simply given by

$$\mathrm{D} = 1/|\boldsymbol{\xi}_{\mathrm{i}}|. \tag{11b}$$

While the derivation of the O-cell walls assumes the existence of an O-point lattice, a representation of a set of O-cell walls with $\mathbf{c}^{\mathrm{O}}_{\beta i}$ defined by Eq. 10a remains valid for O-lines or O-planes if they are periodic. The expressions for dislocations in Eq. 11 are applicable, provided that each of the two areas separated by an O-cell wall trace contains an O-line element or intersected O-line or O-plane element. For example, the dislocation structure in any one of three small angle grain boundaries in Fig. 2 can be calculated with the aforementioned equations for the dislocations, especially in the inclined boundary, for which a simplified formula is not available. In this special case, any of the three interfaces can meet the trace condition, so that the O-cell wall traces in the interface can represent the dislocations.

Depending on the interfacial orientation $\mathbf{n}$ and the number of $\mathbf{b}^{\mathrm{L}}_{\alpha \mathrm{i}}$ to solve $\mathbf{x}^{\mathrm{O}}_{\mathrm{i}}$ for the O-elements intersected by the interface, an interface may contain 0, 1, 2, or 3 sets of periodic interfacial dislocations. Eq. 11 is applicable to each set of dislocations in an interface, by taking the $\mathbf{c}^{\mathrm{O}}_{\beta i}$ corresponding to individual $\mathbf{b}^{\mathrm{L}}_{\alpha i}$. The resultant structure consists of continuous dislocation lines only if the interface contains one or two sets of dislocations. Otherwise, a three-set structure is a network consisting of dislocation line segments stopping at points where three dislocation segments meet. Specially, if an O-plane exists, all $\mathbf{c}^{\mathrm{O}}_{\beta i}$ determined from Eq. 10 will be normal to this O-plane, even though periodic O-planes are not solvable. Then, no intersection line can be obtained if an interface is parallel to the O-plane, leading to a dislocation-free (fully coherent) interface.

In special cases, if $\mathbf{n}$ is perpendicular to $\mathbf{c}^{\mathrm{O}}_{\beta i}$ and $\mathbf{A}$ is an isotropic transformation in 2D, as occurs to symmetric tilt and twist grain boundaries, or an epitaxial interface between two phases of samestructures with slightly different lattice parameters, the expression for the dislocation spacing is particularly simple: $D = 1/|\Delta \mathbf{b}^{*}_{i}|$ [23]. This unified formula can be used to derive different D formulas for simple interfaces in textbooks, e.g., [18]: $D = b/\theta$ for a special small angle (θ) grain boundary and $D = b/\delta$ for an interphase boundary with isotropic misfit (δ), where $b = |\mathbf{b}^{\mathrm{L}}_{\alpha i}|$. The agreement between the unified formula and well-known formulas verifies of the O-cell based expression for dislocations in general interfaces.

When an interface does meet the condition for O-cell wall traces to represent the dislocations, the dislocation structure in the interface can be estimated. For this case, one may decompose the interface into various facets such that the interface is microscopically stepped to pass along O-elements in the adjacent O-cells. Therefore, each local facet meets the trace condition. According to the association between the $\mathbf{x}^{\mathrm{O}}_{\mathrm{i}}$ connecting the adjacent O-elements and the specific O-cell wall $\mathbf{c}^{\mathrm{O}}_{\beta i}$ corresponding to the same $\mathbf{b}^{\mathrm{L}}_{\alpha \mathrm{i}}$, the overall dislocations structures in different portions of facets can be determined with Eq. 11. This concept has been suggested by Bollmann [11], who has illustrated a determination of a complicated dislocation structure in stepped interfaces based on a one-to-one correspondence between points in the b-lattice points (the reference lattice) and the O-points. This general method was seldom utilized by other researchers, probably because the spacing of periodic dislocations is the major concern in most applications and locations of individual dislocations in non-periodic structure are not usually demanded. The concept of b-lattice is also useful if the O-lattice is unavailable in 3D, i.e., when Rank(T) < 3. Bollmann [9] has suggested a projection of b-lattice points in 3D onto a proper

b-subspace. The structure of the two sets of parallel dislocations can be determined this way [25].

A comparison with the Frank–Bilby equation

The O-lattice theory is closely related to the Frank–Bilby equation [19, 20], which is presented in a number books (e.g., [2, 24]) as a major method for calculating interfacial dislocations. Bollmann [9] has considered that the O-lattice theory is based on the Frank model. Christian [17] regarded the O-lattice theory as a quantized version of the Bilby theory. The Frank–Bilby equation can be equivalently expressed as $\mathbf{B} = \mathbf{Tp}$, where $\mathbf{B}$ is the Burgers vector content associated with $\mathbf{p}$, which is a vector in an interface. Comparing the Frank–Bilby equation with Eq. 6, one finds that $\mathbf{B} = \mathbf{T}\mathbf{x}_\beta = \Sigma k_i \mathbf{b}^{L}_{\alpha i}$, if $\mathbf{p} = \mathbf{x}_\beta$. Therefore, mathematically, it is possible that both the Frank–Bilby equation and the O-lattice theory provide identical descriptions of the dislocation structure. In the following comparison one will see the advantage of the O-lattice approach over the Frank–Bilby equation in several aspects.

First, in conventional applications of the Frank–Bilby equation, the overall misfit is presumably accommodated by up to three sets of dislocations with three non-coplanar $\mathbf{b}^{L}_{\alpha i}$ in a system [1, 2, 24]. Usually there are more than three Burgers vectors in a system, and hence there exist multiple ways to decompose a particular $\mathbf{B}$ vector with the components of three Burgers vectors, as also pointed out by Christian [17]. This problem does not exist in the O-lattice approach, which has taken all attainable $\mathbf{b}^{L}_{\alpha i}$ into consideration. Only when the selected interface contains less than three sets of dislocations and when the $\mathbf{b}^{L}_{\alpha i}$ for the dislocations are properly included in the model using the Frank–Bilby equation, can the calculations based on both approaches yield identical results. If the Burgers vectors were not selected properly, the calculation using the Frank–Bilby equation may lead to a wrong dislocation structure.

Secondly, there is no unique description with the Frank–Bilby equation if an interface contains more than three sets of dislocations, as noted by Sutton and Balluffi [2]. This problem has been solved in the framework of the O-lattice. When the direction of $\mathbf{p}$ is arbitrary, the number of types of the Burgers vectors of dislocations across by the given $\mathbf{p}$ in sufficient length may exceed three. Suppose that an O-point lattice exists, and the Burgers vectors can be specified according to the O-cell walls intersected by this $\mathbf{p}$. Specifically, one can decompose $\mathbf{p}$ approximately into $\Sigma k_i \mathbf{x}^{O}_i$, with each vector segment $k_i \mathbf{x}^{O}_i$ passing along the O-cells intersected locally by $\mathbf{p}$ as far as possible. The resultant vector chain linking the overall $\Sigma k_i \mathbf{x}^{O}_i$ segments in the proper order should form a zigzag path in the closest vicinity of $\mathbf{p}$. Since this decomposition of $\mathbf{p}$ into $k_i \mathbf{x}^{O}_i$ is virtually unique, a unique $\mathbf{B} \approx \Sigma k_i \mathbf{b}^{L}_{\alpha i}$ can be calculated according to Eq. 7.

Thirdly, while the dislocation spacing formulas for simple structures can be obtained from both approaches, the geometry of the dislocations is directly related to the Burgers vector of the dislocations in the O-cell based formula, but this is not the case in the formula based on the Frank–Bilby equation. In addition, the derivation based on the O-cell construction is much simpler. For example for a general isotropic transformation, the dislocation spacing can be expressed as $D = 1/|\Delta \mathbf{b}^{*}_i| = |\mathbf{b}^{L}_{\alpha i}||\mathbf{b}^{L}_{\beta i}|/[|\mathbf{b}^{L}_{\alpha i}|^2 + |\mathbf{b}^{L}_{\beta i}|^2 - 2|\mathbf{b}^{L}_{\alpha i}||\mathbf{b}^{L}_{\beta i}|\cos(\theta)]^{1/2}$ [23]. This formula is equivalent to Eq. 2.103 in [2] (after correcting a minor mistake), which has been derived in a more complicated way based on the Frank–Bilby equation.

In summary, both the Frank–Bilby equation and the O-lattice approach are based on the same displacement field to determine the overall misfit. The O-lattice approach provides a detailed method for decomposition of the total misfit into discrete dislocations for a general interface, while the approach based on the Frank–Bilby equation can make proper decomposition mainly in simple cases. Thus, the O-lattice approach has a broader applicability. For simple cases, where both approaches are applicable, the derivation based on the O-lattice is simpler, and the relationship between the Burgers vector and spacing of the dislocations is clearer. Therefore, while the Frank–Bilby equation is broadly appreciated, the advanced O-lattice approach deserves more attention.

Description of singular interfaces with principal O-lattice planes and Δgs

Description of singular interfaces with principal O-lattice planes

Having introduced a method for calculating the dislocation structure based on the O-lattice and O-cell structures, we now return to the issue on identification of singular interfaces. When the effect of dislocations is dominant, a singular interface will contain a dislocation structure that exhibits a singularity feature. As stated earlier, the dislocation structure in a singular interface can be identified comparative to an arbitrary interface in its vicinal IO and OR, in that one or more types of dislocations must be present in the vicinal interface. The number of the types of dislocations in an interface depends on how many sets of O-cell walls are intersected by the interface. The minimum number of dislocations in a singular interface depends on the dimension of the O-elements in the O-lattice constructed at the given OR. Therefore, the candidates for singular interfaces are examined according to different O-elements.

Consider first the case of an O-point lattice. As seen from the above discussions about the Frank–Bilby equation, an arbitrary $\mathbf{p}$ will possibly intersect many sets of dislocations. Only when a line is along a principal O-lattice vector $\mathbf{x}_i^{\mathrm{O}}$, will it constantly intersect a single set of O-cell walls. Therefore, along the direction of $\mathbf{x}_i^{\mathrm{O}}$, there is a single set of dislocations with Burgers vector of $\mathbf{b}_{\alpha i}^{\mathrm{L}}$; along any its vicinal direction one finds one or more other types of dislocations. Clearly, an interface containing two singular directions along different vectors of $\mathbf{x}_i^{\mathrm{O}}$ is fully singular with respect to any variation in the IO. Usually, three $\mathbf{x}_i^{\mathrm{O}}$ may coexist in one plane, corresponding to three coplanar $\mathbf{b}_{\alpha i}^{\mathrm{L}}$. Therefore, in the case where an O-point lattice exists, the minimum number of types of dislocations in a singular interface is either two or three, with coplanar Burgers vectors. Any deviation in the IO will cause additional type(s) of dislocations in a vicinal interface.

In the case where an O-line lattice exists, another singular direction is specified, i.e., the invariant line, $\mathbf{x}_{\mathrm{in}}$. Along $\mathbf{x}_{\mathrm{in}}$, there is no dislocation, and along any of its vicinal direction one finds one or more types of dislocations. For this case, a singular interface must contain this singular direction. The minimum number of types of dislocations in a singular interface is one. The corresponding interface contains the periodic O-lines. The equivalent condition is that the interface must contain $\mathbf{x}_{\mathrm{in}}$ and $\mathbf{x}_i^{\mathrm{O}}$. However, this $\mathbf{x}_i^{\mathrm{O}}$ is not fully singular, since another vector that is a linear combination of $\mathbf{x}_{\mathrm{in}}$ and $\mathbf{x}_i^{\mathrm{O}}$ also intersect a single set of dislocations. Any deviation in the IO from the interface containing the O-lines will cause additional type(s) of dislocations in a vicinal interface. In case where an O-plane exists, obviously, the interface parallel to the O-plane is singular. It contains no dislocation, and any deviation in the IO will cause additional type(s) of dislocations in a vicinal interface. This interface may be considered to contain two $\mathbf{x}_{\mathrm{in}}$ in different directions.

A summary of the possible singular interfaces for different O-elements is given in Table 1. In the table a singular interface is characterized with two singular directions, $\mathbf{s}_1$ and $\mathbf{s}_2$, which can be either $\mathbf{x}_i^{\mathrm{O}}$ or $\mathbf{x}_{\mathrm{in}}$. A singular interface may contain up to three sets of dislocations. The corresponding vicinal interface must contain at least one more set of dislocations. A vicinal interface may contain as low as one set of dislocations. Therefore, except for the singular interface containing no dislocations, it is impossible to identify a singular interface solely according to the number of the sets of dislocations in the interface. Identification of the O-elements helps to clarify the uncertainty. As shown in Table 1, corresponding to each type of O-element, the minimum number of the set of dislocation is defined. Take the O-line lattice in Fig. 2 for example. The singular interface should contain a single set of dislocations. Therefore, the symmetric tilt grain boundary containing a single set of dislocations is a singular interface. The incline and twist boundaries containing two sets of dislocations are not singular interfaces, since a small deviation in the IO will not alter the types of dislocations in these interfaces. However, if the O-lattice is a point lattice, an interface containing two sets of periodic dislocations is a singular interface. The planes containing two or three $\mathbf{x}_i^{\mathrm{O}}$ in an O-point lattice, the plane containing the O-lines, and the O-plane have been named as the principal O-lattice planes for the O-lattice of different O-elements [6]. With this term, it is convenient to conclude that all principal O-lattice planes are the candidates for the singular interfaces.

The singularity argument is consistent with the early assumption by Bollmann and Nissen [8] that the three faces of an O-lattice unit cell, each containing two $\mathbf{x}_i^{\mathrm{O}}$ (in an O-point lattice), are candidates for the optimum interfaces. In their method, only three non-coplanar $\mathbf{x}_i^{\mathrm{O}}$ were taken into consideration. The candidates for the singular interfaces, or optimum interfaces, have been extended here to include all faces, each containing two $\mathbf{x}_i^{\mathrm{O}}$ associated with attainable $\mathbf{b}_{\alpha i}^{\mathrm{L}}$. The total number of the candidates is usually much greater than three [6]. Therefore, when an O-point lattice is constructed, an embedded particle may be fully surrounded by principal O-lattice planes in different orientations when a local interface is allowed to step along these planes. This description in terms of the primary O-lattice planes is in accord to but more restrictive than Bollmann's suggestion that "a crystal boundary will be placed, as far as possible, through O-elements." P. 186 [9]. This suggestion did not specify what neighboring O-elements an interface should pass through. However, one might intuitively understand that an interface should pass through the O-elements in close neighbors, resulting in a preferred interface containing dense O-element. Using the density of the O-elements as optimal

Table 1 Dislocation structures in singular interfaces for different O-elements

O-element	No. of minimum set(s) of dislocations in a singular direction		No. of minimum set(s) of dislocations in a	
	$\mathbf{s}_1$	$\mathbf{s}_2$	Singular interface	Vicinal interface
Point	1 ($\mathbf{s}_1 = \mathbf{x}_1^{\mathrm{O}}$)	1 ($\mathbf{s}_2 = \mathbf{x}_2^{\mathrm{O}}$)	2 or 3 (coplanar $\mathbf{b}_{\alpha i}^{\mathrm{L}}$)	3 (non-coplanar $\mathbf{b}_{\alpha i}^{\mathrm{L}}$)
Line	0 ($\mathbf{s}_1 = \mathbf{x}_{\mathrm{in}}$)	1 ($\mathbf{s}_2 = \mathbf{x}_i^{\mathrm{O}}$)	1	2
Plane	0 ($\mathbf{s}_1 = \mathbf{x}_{\mathrm{in1}}$)	0 ($\mathbf{s}_1 = \mathbf{x}_{\mathrm{in2}}$)	0	1

condition may not always give the principal O-lattice planes. Note that when the misfit strain field is strongly anisotropic, a line along dense O-points may not be parallel to $\mathbf{x}_i^{\mathrm{O}}$ and hence it is not a singular direction to define a singular interface. Here, it is emphasized that a preferred interface should pass the O-elements in contacted O-cells. This equivalently requests a preferred interface to pass the O-elements connected by $\mathbf{x}_i^{\mathrm{O}}$. The resultant overall preferred interface will be locally along singular interfaces defined by the principal O-lattice planes. It is worth of noting that a singular interface containing widely spaced O-elements rather than densely packed ones is probably more energetically favorable due to the low dislocation density in the interface.

Description of singular interfaces with $\Delta\mathbf{g}$s

While the normal of a set of principal O-lattice planes in an O-point lattice can be determined from the cross product of the two $\mathbf{x}_i^{\mathrm{O}}$ in the plane, it is more convenient to specify the plane normal with a reciprocal vector. The reciprocal vector for a set of principal O-lattice planes in the O-point lattice is simply given by a displacement vector in the reciprocal space [13],

$$\Delta\mathbf{g}_{\mathrm{P}-\mathrm{I}} = \mathbf{T}'\mathbf{g}_{\mathrm{P}-\alpha} = \mathbf{g}_{\mathrm{P}-\alpha} - \mathbf{g}_{\mathrm{P}-\beta}, \tag{12}$$

where subscript I indicates that reciprocal vectors $\mathbf{g}_\alpha$ and $\mathbf{g}_\beta$ are related by the following transformation in reciprocal space [17]

$$\mathbf{g}_{\mathrm{P}-\beta} = (\mathbf{A}^{-1})'\mathbf{g}_{\mathrm{P}-\alpha}. \tag{13}$$

Subscript "P" denotes the "principal" level: $\Delta\mathbf{g}_{\mathrm{P\text{-}I}}$ defines the principal O-lattice plane, $\mathbf{g}_{\mathrm{P}\text{-}\alpha}$ defines the principal (low index) planes in lattice α, and $\mathbf{g}_{\mathrm{P}\text{-}\beta}$ is similarly defined. The plane normal to $\mathbf{g}_{\mathrm{P}\text{-}\alpha}$ contains two or three $\mathbf{b}_{\alpha i}^{\mathrm{L}}$ corresponding to the $\mathbf{x}_i^{\mathrm{O}}$ in the plane normal to $\Delta\mathbf{g}_{\mathrm{P\text{-}I}}$. Note that it is implied in Eq. 12 that lattice α is the identification lattice for determining the displacement in reciprocal space. This is different from formula for the displacement in Bollmann's book (Eq. C7-22 in [11]), where identification lattice β was kept for calculation in reciprocal space. For this reason, while Eq. 12 is consistent with Bollmann's formula for reciprocal vector for the O-lattice (Eq. I2–22 in [11]), the identity of $\Delta\mathbf{g}_{\mathrm{P\text{-}I}}$ as a displacement vector was not noticed in the book. Using the reference lattice α as the identification lattice in reciprocal space, it is convenient to test the reciprocal relationship between $\mathbf{x}_i^{\mathrm{O}}$ and $\Delta\mathbf{g}_{\mathrm{P\text{-}I}}$ from [26]

$$\Delta\mathbf{g}_{\mathrm{P}-\mathrm{I}}/\mathbf{x}_{\mathrm{i}}^{\mathrm{O}} = \mathbf{g}'_{\mathrm{P}-\alpha}\mathbf{T}\mathbf{x}_{\mathrm{i}}^{\mathrm{O}} = \mathbf{g}'_{\mathrm{P}-\alpha}\mathbf{b}_{\alpha\mathrm{i}}^{\mathrm{L}} = 0. \tag{14}$$

Therefore, once a singular interface is parallel to a principal O-lattice plane normal to a specific $\Delta\mathbf{g}_{\mathrm{P\text{-}I}}$, the Burgers vectors of the dislocations in the interface are known to lie in the plane normal to the $\mathbf{g}_{\mathrm{P}\text{-}\alpha}$ associated with the $\Delta\mathbf{g}_{\mathrm{P\text{-}I}}$. In the case of an O-point lattice, the standard reciprocal relationship holds between each set of principal O-lattice planes and a reciprocal vector of $\Delta\mathbf{g}_{\mathrm{P\text{-}I}}$. One can specify the total number of principal O-lattice planes according to Eq. 12. Take a bcc lattice as lattice α for example. It is well known that there are six $\mathbf{g}_{\mathrm{P}\text{-}\alpha}$s of $\{110\}_{\mathrm{b}}$, if $\langle 111\rangle_{\mathrm{b}}/2$ are adopted for $\mathbf{b}_{\alpha\mathrm{i}}^{\mathrm{L}}$. Therefore, one finds six sets of principal O-lattice planes, each normal to a $\Delta\mathbf{g}_{\mathrm{P\text{-}I}}$ associated with different $\mathbf{g}_{\mathrm{P}\text{-}\alpha}$ of $\{110\}_{\mathrm{b}}$.

The expression of the principle O-lattice planes with $\Delta\mathbf{g}_{\mathrm{P\text{-}I}}$s facilitates a direct measurement of singular interfaces. The $\Delta\mathbf{g}_{\mathrm{P\text{-}I}}$ vectors can be conveniently determined from an overlapped diffraction pattern taken from an interface region using a transmission electron microscope (TEM) (Ref. Fig. 5). Figure 4a provides an illustration of a diffraction pattern from a zone axis of $[-101]_{\mathrm{f}}$ from a fcc crystal, overlapped with a pattern of $[-1-11]_{\mathrm{b}}$ from a bcc crystal at the Pitsch OR [27]. Three $\Delta\mathbf{g}_{\mathrm{P\text{-}I}}$s associated with $\{110\}_{\mathrm{b}}$ are contained in this pattern. When the related $\mathbf{g}_{\mathrm{P}\text{-}\alpha}$ and $\mathbf{g}_{\mathrm{P}\text{-}\beta}$ are parallel to each other, e.g., $(1-10)_{\mathrm{b}}$ and $(0-20)_{\mathrm{f}}$ in Fig. 4a, the associated $\Delta\mathbf{g}_{\mathrm{P\text{-}I}}$ that is parallel to them is in a rational orientation with respect to both crystals. However, some $\Delta\mathbf{g}_{\mathrm{P\text{-}I}}$s may not be parallel to their connected $\mathbf{g}_{\mathrm{P}\text{-}\alpha}$ or $\mathbf{g}_{\mathrm{P}\text{-}\beta}$, even if the OR is rational, such as $\Delta\mathbf{g}_{\mathrm{P\text{-}I1}}$ and $\Delta\mathbf{g}_{\mathrm{P\text{-}I2}}$ marked in Fig. 4a. In terms of these $\Delta\mathbf{g}_{\mathrm{P\text{-}I}}$s, the reason for irrational orientations of possible singular interfaces become clear. Additionally, a singular interface can also be identified in the TEM images according to the property of the planes defined by $\Delta\mathbf{g}_{\mathrm{P\text{-}I}}$(s). In general, a reciprocal vector $\Delta\mathbf{g}$ (=$\mathbf{g}_\alpha - \mathbf{g}_\beta$) presents a set of periodic Moiré planes formed from the interference of planes defined by $\mathbf{g}_\alpha$ and $\mathbf{g}_\beta$ [28]. The Moiré patterns visible from the TEM images can often be used to verify the association of a facet with any $\Delta\mathbf{g}$ [29] (Ref. Fig. 5). If $\mathbf{g}_\alpha$ and $\mathbf{g}_\beta$ are not parallel to each other, the planes represented by $\mathbf{g}_\alpha$ and $\mathbf{g}_\beta$ will match at their edges in the interface parallel to the Moiré planes [6]. When this matching feature is observed from a high resolution TEM, it can also be used to verify the association between the observed interface and the $\Delta\mathbf{g}$ related to the matching planes.

The expression of the principal O-lattice planes with $\Delta\mathbf{g}_{\mathrm{P\text{-}I}}$s is applicable to the other shapes of O-elements [6]. Only when $\mathrm{Rank}(\mathbf{T}) = 3$, can a one-to-one correspondence be defined between a set of principal O-lattice planes and a reciprocal vector of $\Delta\mathbf{g}_{\mathrm{P\text{-}I}}$. When $\mathrm{Rank}(\mathbf{T}) < 3$, $\Delta\mathbf{g}_{\mathrm{P\text{-}I}}$s are always computable with Eq. 12 and its total number again equals to that of $\mathbf{g}_{\mathrm{P}\text{-}\alpha}$s. However, Eq. 12 is now a projection operation. When $\mathrm{Rank}(\mathbf{T}) = 2$, all resultant $\Delta\mathbf{g}_{\mathrm{P\text{-}I}}$s must lie in a plane normal to the invariant line $\mathbf{x}_{\mathrm{in}}$ [12]. When $\mathrm{Rank}(\mathbf{T}) = 1$, all resultant $\Delta\mathbf{g}_{\mathrm{P\text{-}I}}$s must lie in one direction

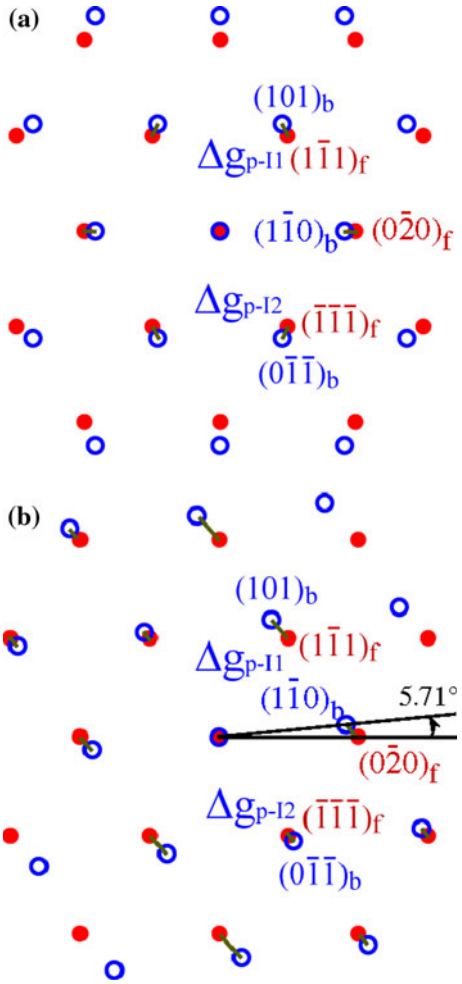

Fig. 4 Overlapped diffraction pattern for hypothetic fcc/bcc systems in zone axes of $[-101]_f//[-1-11]_b$: **a** Pitsch OR with $(0-20)_f//(1-10)_b$, **b** Anticlockwise rotation of 5.71° of bcc from (**a**) to lead to parallelism of $\Delta\mathbf{g}_{p\text{-}Ii}$. *Dots* (*red*) and *circles* (*blue*) represent reciprocal points in lattice α and β, respectively

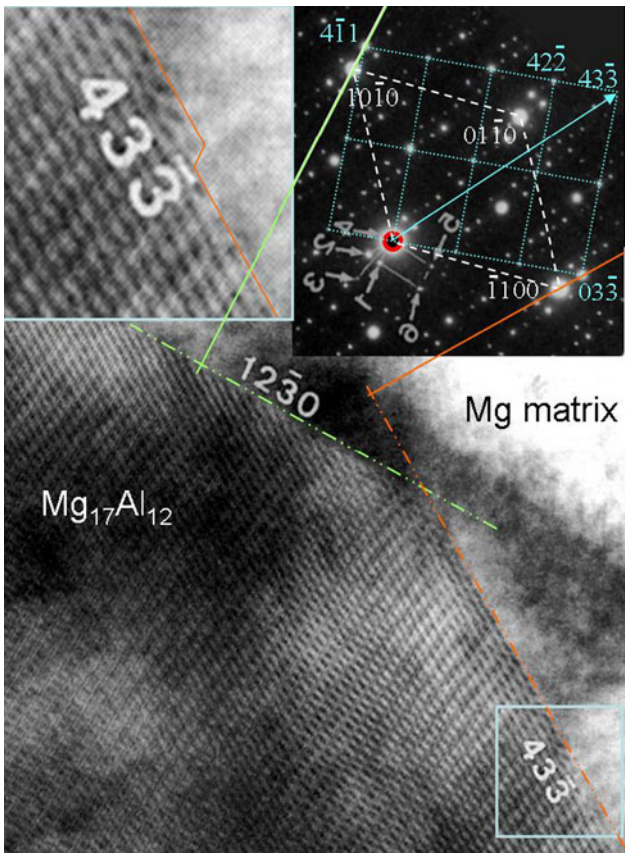

Fig. 5 TEM image of an embedded $Mg_{17}Al_{12}$ plate-shaped precipitate in an AZ91 Mg–Al alloy, viewed from [0001] of the matrix (hcp) and [011] of $Mg_{17}Al_{12}$ (bcc). The terraces in each side facet are parallel to a set of Moiré fringes, normal to a $\Delta\mathbf{g}$ marked in the diffraction pattern in the top-right insert (where diffraction spots from the matrix are indicated with four indexes, and that from $Mg_{17}Al_{12}$ with three indexes). The area near the index "43−3" has been enlarged in the top-left insert to show a ledge between terraces. This figure has reused parts of Figs. 4 and 6 in [29] with kind permission from Taylor & Francis Group (http://www.informaworld.com)

normal to the invariant plane [30]. An O-lattice in 3D is usually unsolvable when Rank(**T**) < 3, but determination of one principal O-lattice plane containing either a set of O-lines or one O-plane element is often possible. This principal O-lattice plane is normal to a group of $\Delta\mathbf{g}_{P\text{-}I}$s. It has been proven [12] that the plane containing a set of O-lines is normal to at least two $\Delta\mathbf{g}_{P\text{-}I}$s, with their associated $\mathbf{g}_{P\text{-}\alpha}$ lying in the zone axis of $\mathbf{b}_i^L$ for the O-lines. Figure 4b shows an example of three parallel $\Delta\mathbf{g}_{P\text{-}I}$s in an overlapped diffraction pattern in the same zone axes as in Fig. 4a. Because of linear relationship between reciprocal vectors in these parallel zone axes, all $\Delta\mathbf{g}_I$s must be parallel to each others. According to the plane matching property of the Moiré planes, the singular interfaces normal to the parallel $\Delta\mathbf{g}_I$s will appear coherent when it is viewed from the orientation parallel to the zone axes in Fig. 4b. This is because the misfit displacement, parallel to the Burgers vector of the dislocations, is along the projection direction and hence invisible. If an O-plane exists, this plane is normal to all $\Delta\mathbf{g}_{P\text{-}I}$s in different zone axes, no mater whether a periodic set of O-planes are available or not. Therefore, any principal O-lattice plane, is normal to at least one $\Delta\mathbf{g}_{P\text{-}I}$. Usually $1/|\Delta\mathbf{g}_{P\text{-}I}|$ only reflects periodicity of the O-point lattice structure, since the O-lines or O-planes do not often display the periodicity in 3D.

In one case, a $\Delta\mathbf{g}_{P\text{-}I}$ does not define a principal O-lattice plane, but it still defines a possible singular interface. This occurs when Rank(**T**) = 2 and when only one set of O-lines is available [25, 31]. The interface normal to a single $\Delta\mathbf{g}_{P\text{-}I}$ contains two sets of parallel dislocations, whose Burgers vectors lie in the plane $\mathbf{g}_{P\text{-}\alpha}$ associated with the particular $\Delta\mathbf{g}_{P\text{-}I}$. This interface is singular with respect to the IO, since any deviation will instigate the formation of one or more extra sets of dislocations. The description of

the dislocation structure in this type of interfaces is complicated, since the O-lattice is not definable in 3D and periodic O-cell structure is unavailable in 3D. Bollmann has provided a method to solve this problem [11]. Since $\Delta\mathbf{g}_{\text{P-I}}$s always exist, the misfit variation can also be analyzed with $\Delta\mathbf{g}_{\text{P-I}}$s regardless of whether the O-elements are solvable in a plane [32]. The relationship defined in Eq. 14 can be extended to more general vectors in the interface [6]. This implies that any misfit displacement in the interface normal to $\Delta\mathbf{g}_{\text{P-I}}$ must lie in the plane normal to $\mathbf{g}_{\text{P-}\alpha}$. Accordingly, one can specify the misfit distribution according to the arrangement of $\Delta\mathbf{g}_{\text{P-I}}$s and their associated Moiré planes [32]. In other cases, an interface may contain two sets of parallel dislocations, such as in an asymmetric tilt grain boundary, which can be added to Fig. 2. This interface is not a singular interface, since a deviation in the IO does not necessarily add new type of dislocations. For the special case in Fig. 1 or 2, each definable $\Delta\mathbf{g}_{\text{P-I}}$ is normal to a principal O-lattice planes containing a set of O-lines. The $\Delta\mathbf{g}_{\text{P-I}}$ associated with the $\mathbf{g}_{\text{P-}\alpha}$ parallel to the rotation axis is a zero vector and it defines the invariant line in reciprocal space.

Finally, we can conclude that the orientation of any singular interface in the primary preferred state, coherent or semicoherent containing 1, 2 or 3 sets of dislocations, can be identified with the $\Delta\mathbf{g}_{\text{P-I}}$ vector(s). In most cases, the singular interface is parallel to a principal O-lattice plane, containing periodically distributed O-points or O-lines, or parallel to an O-plane. Such a singular interface is normal to at least one $\Delta\mathbf{g}_{\text{P-I}}$. An interface containing two set of parallel dislocations is a singular interface if the system only contain one plane of O-lines. This singular interface is normal to one $\Delta\mathbf{g}_{\text{P-I}}$. Only in the case of O-point lattice, the singular interfaces defined by the principal O-lattice planes can fully enclose an embedded crystal. In this case, each $\Delta\mathbf{g}_{\text{P-I}}$ is normal to a set of principal O-lattice planes. Otherwise, the O-plane only confines one singular interface, the resultant shape of embedded phase is a plate. In this case, each $\Delta\mathbf{g}_{\text{P-I}}$ is normal to this O-plane. For the case of O-lines, all possible singular interfaces must contain the invariant line, which is the zone axis of all $\Delta\mathbf{g}_{\text{P-I}}$s. The shape of embedded phase is a lath along the invariant line. The major facet is usually defined by the singular interface containing the O-lines. This interface is normal to a group of $\Delta\mathbf{g}_{\text{P-I}}$s. If only one plane containing the O-lines is available, the rest $\Delta\mathbf{g}_{\text{P-I}}$s also define singular interfaces in various orientations. Therefore, no matter what the dimension is the O-element, an interface that is singular in terms of dislocation defects is always normal to at least one $\Delta\mathbf{g}_{\text{P-I}}$. Reversely, a plane normal to at least one $\Delta\mathbf{g}_{\text{P-I}}$ is always a candidate for a singular interface. Other facets that exhibit singularity in term of ledge defects, i.e., those in rational orientations, may also coexist with the singular interface in terms of dislocation defects considered above.

Considerations on the OR space

In the previous section, the candidates for singular interfaces were mainly analyzed according to the singularity in terms of the dislocation defects with respect to the change in IO. However, these interfaces may not be singular with respect to the OR. Given a system with the freedom to vary the OR, an energetically preferred OR often permits an interface to be singular with respect to the OR. In this section, we discuss the possible preferred ORs.

In the region of space where the OR allows the primary preferred state, one can always construct an O-point lattice at any OR and use $\Delta\mathbf{g}_{\text{P-I}}$s in various orientations to identify a set of semicoherent singular interfaces. These interfaces corresponding to a random OR are not singular with respect to the OR. Restrictions to the OR come from a further reduction of the defects. Here both types of defects—ledges and dislocations—are taken into consideration. If the ledges have a significant effect on the selection of the OR, then the singular interface tends to be parallel to a low index plane, containing densely packed atoms without ledges. The corresponding OR is such that $\Delta\mathbf{g}_{\text{P-I}}$ is parallel to either one or both of $\mathbf{g}_{\text{P-}\alpha}$ and $\mathbf{g}_{\text{P-}\beta}$, to permit the singular interface to characterize singularities in terms of both local minimum dislocations and ledges on the interface plane at least with respect to one crystal. Such an interface has been identified by following one of three $\Delta\mathbf{g}$ parallelism rules, i.e., Rule I in form of $\Delta\mathbf{g}_{\text{P-I}}//\mathbf{g}_{\text{P-}\alpha}$ or $\mathbf{g}_{\text{P-}\beta}$ [6]. Parallelism of two vectors confines two degrees of freedom in the OR space. This means an interface following Rule I is singular with respect to changes in a specific 2D space in the 3D OR space. Usually, a typical rational OR implies parallelism to hold both between $\mathbf{g}_{\text{P-}\alpha}$ and $\mathbf{g}_{\text{P-}\beta}$, and between two low index directions (often $\mathbf{b}^{\text{L}}_{\alpha i}//\mathbf{b}^{\text{L}}_{\beta i}$) in the parallel planes defined by $\mathbf{g}_{\text{P-}\alpha}$ and $\mathbf{g}_{\text{P-}\beta}$. These two pairs of mutually dependent parallel directions fully constrain the OR.

When the singularity in the dislocation structure has a dominant effect, the preferred OR tends to permit the elimination of one or more sets of dislocations, or equivalently the existence of an O-plane or a set of O-lines. However, this demands the system to meet certain conditions. Christian has provided simple criteria to check the conditions [17]. In accordance with the proper lattice correspondence for the primary preferred state, one can determine a unique pure deformation, and three eigenvalues λ_i for this deformation ($\lambda_1 < \lambda_2 < \lambda_3$). If $\lambda_1 < 1$ and $\lambda_3 > 1$, then an invariant line strain ($\text{Rank}(\mathbf{T}) = 2$) is

possible. If $\lambda_1 < 1$, $\lambda_2 = 1$ and $\lambda_3 > 1$, then an invariant plane strain (Rank($\mathbf{T}$) = 1) is possible. Satisfaction to the above condition is independent of the OR but depends on the lattice parameters of the given system.

The condition for the existence of an invariant line can often be fulfilled in commonly used systems. In this case, the OR permitting the invariant line can be searched with the condition of $|\mathbf{T}| = 0$. In the 3D space for the ORs, a surface defined by $|\mathbf{T}| = 0$ can be determined numerically, as shown by Bollmann and Nissen's pioneering analysis [8]. To identify the OR that meets the O-line criterion, one can check angles between any two $\Delta\mathbf{g}_{\text{P-I}}$s, since the plane containing the O-lines is normal to two $\Delta\mathbf{g}_{\text{P-I}}$s. This condition defined another $\Delta\mathbf{g}$ parallelism rule, i.e., Rule II: $\Delta\mathbf{g}_{\text{P-I}i}//\Delta\mathbf{g}_{\text{P-I}j}$ [6]. Analytical method is now available for solving all possible ORs and the corresponding IOs for the interfaces that obey Rule II in an fcc/bcc system [33]. The OR for a particular $\mathbf{b}^{\text{L}}_{\alpha i}$ that defines one type of O-line only confines a curve in the $|\mathbf{T}| = 0$ surface [12]. This means the interface containing the O-lines is singular with respect to the deviation of the OR in 2D, i.e., from the specific curve, but one degree of freedom remains unfixed in the 3D OR space.

Since the direction of two parallel $\Delta\mathbf{g}_{\text{P-I}}$s is usually in an irrational orientation, as seen in Fig. 4b, elimination of one or two sets of dislocations in the singular interface usually comes at the expense of adding ledges to the interface. The viewpoint of ledges replacing dislocations is similar to the concept of the structural ledge model [34], in which the structural ledges may effectively compensate interfacial misfit along one direction. The structural ledge model usually starts from a rational OR with parallel $\mathbf{g}_{\text{P-}\alpha}$ and $\mathbf{g}_{\text{P-}\beta}$. However, a rotation between $\mathbf{g}_{\text{P-}\alpha}$ and $\mathbf{g}_{\text{P-}\beta}$ is necessary for the ledges from different side of the interface to match when the ledge heights ($1/|\mathbf{g}_{\text{P-}\alpha}|$ and $1/|\mathbf{g}_{\text{P-}\beta}|$) are different. Only when such a small rotation (which must agree with Rule II) is allowed, can the structural ledge structure be extended endlessly along the invariant line crossing the ledges [32]. Therefore, an OR which obeys Rule II is usually irrational, but the deviation from a rational OR may be so small that it is often regarded as a measurement error.

Further reduction of defects of either ledges or dislocations requires the OR to obey the $\Delta\mathbf{g}_{\text{P-I}}$ parallelism rule twice: Obeying Rule I and II will lead to a single set of dislocations in a ledge-free interface. Obeying Rule II twice will assure a dislocation-free structure, i.e., an O-plane, in an interface. Parallelism between four independent reciprocal vectors virtually fixes four degrees of freedom, which is usually impossible in the 3D OR space. That is why these conditions can only be fulfilled when the lattice parameters are special, as they bring additional degrees of freedoms to a system with the variation of lattice parameters. When this becomes possible, the OR for either case is a unique point in the $|\mathbf{T}| = 0$ surface. Therefore, the interface free of any dislocation is fully singular in the 5D BGP space. The same is an interface containing a single set of dislocations and no ledges. However, due to the special requirement on the lattice parameters for a fully singular interface, such types of singular interfaces are rare.

In a general system, a further reduction of a set of defects in a plane containing the O-lines is impossible. Therefore, usually singularity in terms of the dislocations only confines four degrees of freedom in the geometry of the singular interface in the 5D BGP space. The observation of reproducible OR indicates that the remaining one degree of freedom in the OR is often fixed by a supplementary constraint. When the supplementary constraint does not correspond to a sharp reduction in the interfacial energy, possible small scattering in the OR may exist. Various supplementary constraints have been used in different models with certain experimental supports, as summarized in a recent review [6]. One supplementary constraint is maximum dislocation spacing, implying a further reduction of energy by minimizing dislocation density. This constraint is in principle consistent with the energy parameter p given by Bollmann and Nissen's [8]. In contrast to the use of a scalar parameter, the present approach directly requires the singularity, equivalent to infinite spacing for other types of dislocations, and the maximization of the spacing of existing dislocations is required at the supplementary level. In the calculation for p, the O-cell walls for the dislocation structure were assumed to be parallel to the faces of the O-lattice unit cell for simplicity [8]. A more strict O-cell calculation is used here.

Another frequently used supplementary constraint is the requirement of $\mathbf{b}^{\text{L}}_{\alpha i}//\mathbf{b}^{\text{L}}_{\beta i}$ in the interface. Such a requirement may be considered to further reduce the interfacial energy by minimizing the ledge energy when ledges must be present. This is because these parallel Burgers vectors, as the common direction between the interface and the terrace planes of the ledges structure, define the direction of the ledges. A ledge along $\mathbf{b}^{\text{L}}_{\alpha i}//\mathbf{b}^{\text{L}}_{\beta i}$ is free of kinks, and hence the distorted bonds associated with the ledge is minimized. Analytical expressions for the ORs, IOs and dislocation structures for the singular interfaces in this condition have been developed for fcc/bcc system and general systems [35, 36]. For this special case, the OR and IO of the singular interface can also be predicted with 2D invariant line model [37] and an edge-to-edge matching model [38], for a selected pair of $\mathbf{b}^{\text{L}}_{\alpha i}//\mathbf{b}^{\text{L}}_{\beta i}$. Under the special condition of $\mathbf{b}^{\text{L}}_{\alpha i}//\mathbf{b}^{\text{L}}_{\beta i}$, the parallel $\Delta\mathbf{g}_{\text{P-I}}$s can be defined in these parallel zone axes, as in Fig. 4b. The singular interface normal to two or

three $\Delta\mathbf{g}_{\text{P-I}}$s will exhibit an edge-to-edge matching feature according to the property of Moiré planes. This matching property has been used as a criterion in the edge-to-edge matching model [7, 38]. In this model, the priority is parallelism of a row of atoms of small misfit, such as along parallel $\mathbf{b}^{\text{L}}_{\alpha i}$ and $\mathbf{b}^{\text{L}}_{\beta i}$. In contrast, in the present approach the parallelism of $\Delta\mathbf{g}_{\text{P-I}}$s is the priority, which ensures singularity, but parallelism of $\mathbf{b}^{\text{L}}_{\alpha i}$ and $\mathbf{b}^{\text{L}}_{\beta i}$ is required at the supplementary level.

Interfaces in a secondary preferred state

According to classification based on coherency in the interfacial structure, a singular interface that is singular in terms of dislocation defects may have three kinds of structures: coherent, semicoherent, and CS-coherent. The aforementioned analyses have yielded a simple method to identify coherent and semicoherent singular interfaces. Namely, they can be identified with measurable $\Delta\mathbf{g}_{\text{P-I}}$ vectors. In this section, it will be shown that any CS-coherent singular interface can also be identified with measurable $\Delta\mathbf{g}$ vectors.

To study a CS-coherent interface, it is crucial to identify the secondary preferred state in the interface. As stated earlier, a secondary preferred state can be represented by a plane of densely and regularly distributed CSL points. Consider first an extreme case, in which an ideal CSL is definable in 3D without imposing any constraint. Therefore, singular interfaces in various orientations can be defined by different planes containing dense CSL points. Each of these CSL planes must be normal to a group of small $\Delta\mathbf{g}$s [39]. This condition stems from the reciprocal theorem proposed by Grimmer [40] between the CSL and DSC lattice (complete pattern shift lattice [11]) in reciprocal space, because any $\Delta\mathbf{g}$ is a vector of the DSC lattice. Although this ideal CSL is uncommon in heterophase systems, if it occurs, any singular interface in the system is normal to measurable $\Delta\mathbf{g}_{\text{CSL}}$'s vectors.

A deviation from a properly selected secondary preferred state usually exists, and this defines the secondary misfit. The secondary misfit dislocation structure can be determined in the same way as the "primary" misfit dislocations based on the O-lattice. All formulas in the O-lattice calculation for interfaces in the primary preferred state can be extended to interfaces in secondary preferred states. To distinguish the preferred state, the adjective "secondary" is used for variables in the calculation of the secondary O-lattice. A construction of the secondary deformation matrix $\mathbf{A}^{\text{II}}$ is essential, and this aspect has been discussed in Selection of $\mathbf{A}$ Section. Based on it the secondary displacement field $\mathbf{T}^{\text{II}}$ can be calculated (Eq. 3). To ensure the relaxed pattern of a selected CSL for a secondary preferred state to be repeated in different regions separated by the secondary dislocations, the secondary Burgers vectors $\mathbf{b}^{\text{II}}$ should be chosen from small lattice translation vectors in the DSC lattice, corresponding to the selected CSL [11]. By replacing $\mathbf{T}$ and $\mathbf{b}^{\text{L}}_{\alpha i}$ with $\mathbf{T}^{\text{II}}$ and $\mathbf{b}^{\text{II}}_{\alpha i}$ in Eqs. 7 and 10, the secondary O-lattice and O-cell structure can be determined. Similarly, by replacing $\mathbf{g}_{\text{P-}\alpha}$ with $\mathbf{g}^{\text{II}}_{\alpha}$ which defines a plane containing two $\mathbf{b}^{\text{II}}_{\alpha i}$, one obtains a $\Delta\mathbf{g}_{\text{P-II}}$ that defines a principal O-lattice plane in a secondary O-point lattice. Like in the cases of primary preferred state, a principal O-lattice plane containing secondary O-lines will be normal to a group of $\Delta\mathbf{g}_{\text{P-II}}$s and a principal O-lattice plane parallel to a secondary O-plane will be normal to all $\Delta\mathbf{g}_{\text{P-II}}$s.

These principal secondary O-lattice planes are the candidates for the singular interfaces, provided that each of the principal secondary O-lattice planes is also parallel to the plane defining the secondary preferred state. Such a singular interface follows $\Delta\mathbf{g}$ parallel Rule I [6], in the form of $\Delta\mathbf{g}_{\text{P-II}}//\mathbf{g}_{\text{CSL}\alpha}//\mathbf{g}_{\text{CSL}\beta}$, where $\mathbf{g}_{\text{CSL}\alpha}$ and $\mathbf{g}_{\text{CSL}\beta}$ define the overlapped planes to form the 2D constrained CSL for the preferred state. It is free from the ledges with terraces parallel to the 2D CSL plane. To distinguish these ledges from other interfacial ledges, we will call them the specific ledges. Usually in the relaxed structure at least a row of atoms from each crystal will be parallel to each other to define a row of dense constrained CSL point. This parallelism condition together with Rule I make the OR to be fixed fully. The corresponding singular interface is normal to the parallel $\mathbf{g}_{\text{CSL}\alpha}$, $\mathbf{g}_{\text{CSL}\beta}$ and $\Delta\mathbf{g}_{\text{P-II}}$. If the interface contains secondary O-lines, the interface will be normal to a group of $\Delta\mathbf{g}_{\text{P-II}}$s. This is classified as another $\Delta\mathbf{g}$ parallelism rule, i.e., Rule III [6] in the form of $\Delta\mathbf{g}_{\text{P-II}i}//\Delta\mathbf{g}_{\text{P-II}j}$. Therefore, a singular interface that is free of any specific ledges and that contains secondary O-lines will follow both Rule I and III. As explained earlier, such an interface is possible only when the lattice parameters of different crystals are specially related. In a more special case, a singular interface is parallel to a secondary O-plane. This interface can be equivalently described as an ideal CSL in 2D, without any secondary strain. Then, the singular interface is normal to all $\Delta\mathbf{g}_{\text{P-II}}$s, and also to $\mathbf{g}_{\text{CSL}\alpha}$ and $\mathbf{g}_{\text{CSL}\beta}$. As expected, the lattice parameters must be specially related for this ideal CSL plane to be realized.

While parallelism of $\mathbf{g}_{\text{P-}\alpha}$ and $\mathbf{g}_{\text{P-}\beta}$ usually ensures $\Delta\mathbf{g}_{\text{P-I}}//\mathbf{g}_{\text{P-}\alpha}//\mathbf{g}_{\text{P-}\beta}$ for a singular interface at the primary preferred state, parallelism of $\mathbf{g}_{\text{CSL}\alpha}$ and $\mathbf{g}_{\text{CSL}\beta}$ to form a plane of constrained CSL does not always permit $\Delta\mathbf{g}_{\text{P-II}}$ to be parallel to these parallel $\mathbf{g}_{\text{CSL}\alpha}$ and $\mathbf{g}_{\text{CSL}\beta}$. This is because the secondary O-lattice and the constrained CSL for the preferred state are independently constructed. For example,

the energetically favorable Burgers vectors $\mathbf{b}^{\mathrm{II}}_{\alpha i}$s for the secondary dislocations may not lie in the constrained CSL plane defined by $\mathbf{g}_{\mathrm{CSL}\alpha}$ and $\mathbf{g}_{\mathrm{CSL}\beta}$. When the condition of $\Delta\mathbf{g}_{\text{P-II}}//\mathbf{g}_{\mathrm{CSL}\alpha}//\mathbf{g}_{\mathrm{CSL}\beta}$ is not reachable, an interface that is singular in terms of secondary dislocations may still tend to be normal to at least one $\Delta\mathbf{g}_{\text{P-II}}$, but the resultant interface may contain specific ledges. In the analysis for the primary preferred state, the interfacial ledges were not taken into consideration. Since the secondary preferred state is defined by a structure in 2D, any specific ledges, where the preferred state discontinues, should be treated physically as secondary dislocations. Corresponding to a selected CSL in 2D, the misfit in the plane is fixed, but $\mathbf{A}^{\mathrm{II}}$ may vary with the assumed CSL in 3D for the calculation of the secondary misfit in 3D. Therefore, the specific ledges may or may not be described by secondary dislocations according to the secondary O-lattice calculation based on the selected $\mathbf{A}^{\mathrm{II}}$. This aspect needs special attention in analysis of singular interfaces in a secondary preferred state.

When a singular interface contains specific ledges, its orientation can be analyzed with two singular directions. One direction is along the ledges. It is usually parallel to a row of dense atoms from each crystal, in the condition that the overlapped rows define a row of dense CSL points constrained with small secondary misfit [15, 16]. Usually a proper $\mathbf{b}^{\mathrm{II}}_{\alpha i}$ and $\mathbf{x}^{\mathrm{II-O}}_{i}$ can be defined along this direction. Thus, a line along this singular direction only intersects up to one set of secondary dislocations [16]. Another singular direction is across the ledges, often being perpendicular to the ledges. The misfit along this singular direction is fully accommodated by the displacement associated with the specific ledges, such that the ledges virtually serve as secondary misfit dislocations. Depending on the selection of $\mathbf{A}^{\mathrm{II}}$, this direction can be defined by either the secondary invariant line $\mathbf{x}^{\mathrm{II}}_{\mathrm{in}}$ or by a principal vector of secondary O-lattice $\mathbf{x}^{\mathrm{II-O}}_{i}$. When this singular direction is defined by $\mathbf{x}^{\mathrm{II}}_{\mathrm{in}}$, the secondary misfit displacement associated with the ledges crossed by a line along $\mathbf{x}^{\mathrm{II}}_{\mathrm{in}}$ can fully cancel the secondary misfit in the terraces crossed by the line. When this singular direction is defined by $\mathbf{x}^{\mathrm{II-O}}_{i}$, each specific ledge is associated with the secondary dislocation, that accommodates the secondary misfit strain field between the secondary O-elements connected by $\mathbf{x}^{\mathrm{II-O}}_{i}$. In both cases, any deviation from this singular direction in terms of either $\mathbf{x}^{\mathrm{II}}_{\mathrm{in}}$ or $\mathbf{x}^{\mathrm{II-O}}_{i}$ implies additional type of secondary dislocations in the interfaces.

The one-to-one association between a specific ledge and a secondary dislocation is ensured by the geometry of the interface being normal to a group of specially arranged parallel $\Delta\mathbf{g}$s [6]. Since in both cases the ledges play a role in cancellation of the secondary misfit, the line along $\mathbf{x}^{\mathrm{II-O}}_{i}$ can be treated as a quasi invariant line [41]. Therefore, due to the presence of either the secondary invariant line or the quasi invariant line, it is possible to find a group of parallel $\Delta\mathbf{g}$s in the zone axis along the ledges. The corresponding singular interface is said to obey $\Delta\mathbf{g}$ parallelism Rule III: in the form of either $\Delta\mathbf{g}_{\text{P-II}i}//\Delta\mathbf{g}_{\text{P-II}j}$ or $\Delta\mathbf{g}_{\text{P-II}}//\Delta\mathbf{g}_{\text{CSL-r}}$, which is more specific than Rule III in the early version [6]. Here, $\Delta\mathbf{g}_{\text{CSL-r}}$ is recovered from $\Delta\mathbf{g}_{\mathrm{CSL}}$ that defines the plane for the preferred state in the constrained CSL. Any deviation in the OR will destroy the special correspondence between the secondary dislocations and ledges, or destroy the existence of $\mathbf{x}^{\mathrm{II}}_{\mathrm{in}}$ in the interface, and hence cause additional defects to be present. Therefore, the CS-coherent interface containing the specific ledges that can fully cancel secondary misfit is fully singular with respect to both IO and OR. Similar to the primary preferred state, the OR allowing for Rule III can be determined with condition of $|\mathbf{T}| = 0$. In this case with a pair of parallel directions along the ledge, the calculation can be made in 2D within the plane normal to the ledge. Examples about how to select the constrained CSL and how to calculate the OR and IO can be found in [15, 41].

Finally, an example of a singular CS-coherent interface in an AZ91 Mg alloy [29] is given in Fig. 5 to demonstrate the relationship between interface facets and $\Delta\mathbf{g}$s. This example is helpful because the Moiré fringes due to overlapping to the two crystals can be clearly seen. These fringes can be used to test the relationship between interface facets and $\Delta\mathbf{g}$s. TEM image in Fig. 5 shows two interface facets between an embedded $Mg_{17}Al_{12}$ (bcc) precipitate plate in the matrix (hcp). As shown in the inserted diffraction pattern, the OR between the two phases is close to the Burgers OR, described by $(0001)_{\mathrm{M}}//(011)_{\mathrm{P}}$ and $[01-10]_{\mathrm{M}}//[21-1]_{\mathrm{P}}$, where subscripts "M" and "P" denote matrix and precipitate, respectively. One can also see from the index in this diffraction pattern that the lattice parameters of the two lattices differ significantly ($a_{\mathrm{P}}/a_{\mathrm{M}} \approx 3$) (Many other spots are due to double diffraction). Therefore, the singular interface in this system must be in a secondary preferred state. According to original study of this system [29], the broad face of the plate is parallel to $(0001)_{\mathrm{M}}$ and $(011)_{\mathrm{P}}$. The plate has two faceted side faces of different sizes. The major side face is approximately parallel to $(43-3)_{\mathrm{P}}$ and the minor one is approximately parallel to $(12-30)_{\mathrm{M}}$, as marked in the figure. Each of these faces (or more precisely, the fine facets on the side face) is normal to a $\Delta\mathbf{g}$ in the inserted diffraction pattern (i.e., $(43-3)_{\mathrm{P}}$ side face is normal to $(-1100)_{\mathrm{M}}$–$(03-3)_{\mathrm{P}}$, and $(12-30)_{\mathrm{M}}$ side face is normal to $(10-10)_{\mathrm{M}}$–$(4-11)_{\mathrm{P}}$). This relationship can be verified by the Moiré fringes in the image, since the fine facets in each side face are exactly parallel to a set of Moiré fringes, which must be normal to the corresponding $\Delta\mathbf{g}$ [28]. A careful examination [29] revealed that

the $(43-3)_P$ side face is normal to a group of $\Delta\mathbf{g}$s. A more detailed study [16] has shown that the parallel $\Delta\mathbf{g}$s include a $\Delta\mathbf{g}_{P\text{-}II}$ $(=(02-20)_M-(63-3)_P)$ and a $\Delta\mathbf{g}_{CSL\text{-}r}$ $(=(-1100)_M-(03-3)_P)$, indicating that the major side face obeys Rule III. This study has also provided the configuration of secondary dislocations of the CS-coherent structure in this major side face [16].

As seen from Fig. 5, the observed faceted interfaces in high index or irrational orientations may appear puzzling. The use of $\Delta\mathbf{g}$s provides a convenient and effective tool to rationalize these puzzling facets before any calculation is made. Parallelism of $\Delta\mathbf{g}$s may not be obvious in the limited range of a diffraction pattern, and the special OR for the parallelism of $\Delta\mathbf{g}$s may be buried in the experimental uncertainty, as in the case of Fig. 5 (where a rotation of $\sim 0.5°$ from the Burgers OR was found [29]). To examine the possible CSL in reciprocal space and parallelism of $\Delta\mathbf{g}$s, one is advised to draw points of overlapped reciprocal lattices in a large range. Examples for this practice can be found in [15, 16].

Discussions

On identities and roles of ledges and dislocations

In this article, ledges and dislocations are identified according to their references. Namely, the ledges are defined with respect to the plane of terraces, and dislocations are defined with respect to the continuity of the preferred state. Since the secondary preferred state is defined by a 2D structure, a specific ledge in a CS-coherent interface can be regarded as a secondary dislocation when the terrace plane is parallel to the plane of the constrained CSL that defines the preferred state. It is possible to define the Burgers vector of this secondary dislocation associated with a specific ledge by deliberate selection of the constrained CSL in 3D. An atomic ledge in a semicoherent interface does not usually coincide with a dislocation, whose Burgers vector is common to that of dislocations in either lattice. In general, the row of atoms along a ledge may be associated with local misfit displacement(s). This feature was considered as a characteristic of a dislocation, and called disconnections by Pond and his colleagues in a topological model [42, 43]. It is worth to note that the displacement vectors associated with the individual atoms along a ledge are not identical to a unique effective Burgers vector unless the terrace plane is a true invariant plane such as a twining dislocation. The notation of coherency and anti-coherency dislocations by Olson and Cohen [44] is helpful for clarifying the confusion on the ledges and dislocations. The dislocation defects in a semicoherent interface are anti-coherency dislocations. The disconnections are the coherency dislocations associated with atomic ledges. Such a disconnection in a coherent or semicoherent interface is treated as an atomic ledge but not a dislocation in the present analysis of defect singularity.

When the singular interface is defined according to the singularity in terms of ledges, the singular interface is free of any atomic ledge, and the vicinal interface with its IO deviated from the singular interface will contain the ledges. Like the role of ledges in a surface, these ledges may be referred to as growth ledges, since migration of the singular interface may be assisted by lateral motion of ledges in a vicinal interface. When the singular interface is defined according to the singularity in terms of dislocations, the vicinal interface with its IO deviated from the singular interface will probably also contain ledges. As mentioned earlier, a preferred interface tends to step along the principal O-lattice planes (Ref. the top-left inset in Fig. 5). In this case, the terrace plane is the singular interface. The ledge is associated with one or more misfit dislocations, which cancels the misfit strain associated with the ledge. These dislocations are the extra dislocations necessary in the vicinal interface. The height of such a ledge is usually in unit of $1/|\Delta\mathbf{g}|$. When the O-lattice is a point lattice, each terrace can lie on a position of a set of principal O-lattice planes if the interplanar spacing is $1/|\Delta\mathbf{g}_{P\text{-}I}|$. When the singular interface is defined by a plane containing a set of O-lines or an O-plane, some residual long-range strain may coexist with the dislocation(s) associated with the ledge connecting the singular interfaces at two levels. This is because only one plane containing the O-lines or an O-plane is definable. A displacement with a long-range effect at a ledge can make the same structure to be realized in another terrace. These ledges are possibly movable, so they may serve as growth ledges. When the terrace plane has an irrational orientation, the terrace planes themselves must contain ledges in atomic scale. These atomic ledges are a part of the interfacial structure in the singular interface, and they cannot move individually. Therefore, examination of the terraces according to the singularity of structure in the terrace plane helps one to clarify the mobility and role of ledges.

On limitations of the method

As a geometric approach, the present approach provides a simple and general quantitative method to identify the candidates of singular interfaces. It mainly helps one to understand the observed facets and their related OR. The observation of reproducible OR and facets in irrational IO usually indicates that the preferred facets can be interpreted according to singularity in terms of dislocations. However, this approach is incapable of predicting what would be observed. Application of the approach assumes the lattice misfit distribution play an influential role in the development of the OR and IO. With this assumption, uncertainties in

several levels of inputs still impede the predictability of this approach.

Firstly, the preferred state is an important input for the calculation, but its selection is not always obvious. Identification of the region in the 3D space for the ORs in which the interfaces are in the primary preferred state is relatively easy if this preferred state is allowed by the lattice parameters, such as fcc/bcc system (Fig. 4). This can be done by the construction of one-to-one lattice correspondence in the condition that the deformation from one lattice to the other is reasonably small. The possible ORs for the singular interfaces in the primary preferred state are usually limited to one small region in the 3D space for the ORs, where the misfit strain is small. Usually, a secondary preferred state is adopted when the primary preferred state is not attainable. However, identification of the possible regions in the 3D space for the ORs in which the interfaces are in a plausible secondary preferred state is a difficult task. It was noted by Bollmann [11] that which secondary preferred state is realized in an interface depends on the material and conditions for the interfaces to develop. An investigation of the singular CS-coherent interface often needs guidance from observations for suggestion of the secondary preferred state [15, 16]. Within the region where a preferred state is possible, there are still numerous ORs for candidates of singular interfaces. However, similar to the cases for grain boundaries [45], misorientation range for a CS-coherent interface is much narrower than that for a semicoherent interface. After the preferred state has been decided, the candidates of singular interface can be greatly reduced by the constraint of one or more $\Delta\mathbf{g}$ parallelism rules.

Secondly, which $\Delta\mathbf{g}$ parallelism rule that a system may follow is not predicable according to a geometric analysis. The OR developed in a system is greatly affected by the weight of ledges as defects in the interface. A singular interface according to singularity in terms of ledge defects must be normal to at least one low index $\Delta\mathbf{g}_{\mathrm{P}}$ in one phase, and one in terms of dislocation defects must be normal to at least one $\Delta\mathbf{g}_{\mathrm{P\text{-}I}}$ (or $\Delta\mathbf{g}_{\mathrm{P\text{-}II}}$). When a reproducible OR is observed, the misfit dislocations must play a role in its development. The corresponding singular interface may be attributed to singularity in terms of solely dislocations or an integrated influence of both ledges and dislocations. A preference of $\Delta\mathbf{g}$ parallelism Rule II belongs to the former case. It usually yields a singular semicoherent interface in an irrational orientation, which implies that the energy of ledges is relatively low. The singular interface following Rule I exhibits singularity in terms of both ledge and dislocation defects. In reality, the relative effects of atomic ledges and misfit dislocations may vary from one system to another, depending on the relative energy of these defects. Available data of Wulff plot or surface energy may be used to estimate the effect of ledges on the surface of each crystal. If the cusps in the plot are deep or surface energy is strongly anisotropic, such as for a covalent crystal, then the ledge energy is likely relatively high and one will expect the OR to follow Rule I rather than II. In metallic systems the ledge energy is relatively low [14], and hence obeying Rule II can be expected so that the dislocation set can be minimized, as suggested by observation of irrational habit planes in systems containing fcc, bcc and hcp metallic phases [6]. In a CS-coherent interface, the specific ledges are equally important as the secondary dislocations. In the development of the OR for this interface, both specific ledge and dislocation defects may play a role. Since the specific ledges are usually associated with high energy, a CS-coherent interface has a stronger preference to Rule I than a coherent or semicoherent interface. Following Rule III that yields coincidence of specific ledges and misfit dislocations in a singular interface indicates that the energy of dislocations in the ledge-free singular interface is high due to lack of favorable Burgers vectors in the plane. In general, a singular interface that follows Rule I is relatively easy to understand, as the familiar principle for singular surface also applies. When a singular interface is found to follow a single Rule II or III, one can expect the role of dislocations has overridden the role of ledges in the minimization of interfacial energy. Reversely, if one expects the dislocations to have a dominant role in the development of the OR and singular interface, the system may follow Rule II or III.

Thirdly, even if the rule to be obeyed is known, there are still two types of uncertainties. One is the specific vectors for defining the rule. For example, it concerns what pair of $\Delta\mathbf{g}_{\mathrm{P\text{-}I}}//\mathbf{g}_{\mathrm{P\text{-}}\alpha}$ should be chosen for Rule I, or what $\mathbf{b}^{\mathrm{L}}_{\gamma i}$ should be used to define the O-line in the interface that follow Rule II. After the above vectors are determined, the geometry of candidates of singular interface is confined in a line (possibly a curved line) in the 5D BGP space. Unless simultaneously following two rules is possible, which uniquely fixes a singular interface at one point in 5D BGP space, one will encounter another type of uncertainties. This is the supplementary constraint that a system tends to take. With this supplementary constraint, the candidates for the singular interfaces can be narrowed to one point in the 5D BGP space. Which supplementary constraint a system may select remains to be a challenge. More experimental studies are required to reveal the principles that govern the selection.

The calculation of the dislocation structures with the O-lattice theory is based on an assumption that the misfit is accommodated fully by the dislocations. Without this assumption, the dislocation description of an interface of a particular OR and IO cannot be unique. Consequently, the calculation results are valid for interfaces where any long-range strain, should it exist, is negligibly small. In real

system, a small long-range strain may be present, especially when the interface area is small. Therefore, the interface surrounding a small particle may be free of any dislocation, though misfit from the primary or secondary preferred state exists. Similarly, other singular interfaces with semicoherent or CS-coherent structure may be present with small long-range strain. In particular, the dislocation spacing in a semicoherent or CS-coherent interface may not reach the theoretical value determined from the condition of full accommodation. Usually, the observed spacing may be smaller than the theoretical value. In addition, even though the misfit strain is fully cancelled by the dislocations, the dislocations may not be arranged in even spacing. Small discrepancies at various locals are expected, since the detailed mismatching distribution and local relaxation in different O-cells are usually different. Therefore, the average measured spacing should be used in comparison with the calculated results.

The use of one $\Delta\mathbf{g}$ parallelism rule plus a supplementary constraint can effectively reduce the geometry of the potential singular interfaces to a limited number of isolated points in the 5D BGP space. The structures in these candidates of singular interfaces are different. The present approach does not compare the dislocation structures in different singular interfaces. Even if the dislocation has a predominant effect on the development of the singular interfaces, it is unreasonable to compare the interfacial energy on the basis of the dislocation spacing only. Usually, the dislocation density is high and the core energy of the dislocations should be carefully evaluated. This task attempts to find a global energy minimum, which is usually beyond the capacity of a geometrical model. Finding the global energy minimum requires a physical model. Compared with searching for local minima in the whole 5D BGP space with a physical model, the candidates of singular interfaces identified from the present geometric analysis can greatly reduce the calculations for energy. In further study, the results from this approach will be used as input for calculating interfacial energy. In addition, detailed investigations are required to find how mobility of a singular interface and possible long-range strain may affect the selection of the OR, which has been the major concern in the PTMC [21].

Summary

Based on the assumption that singularity in interfacial energy is associated with singularity in the defect structure in an interface, singular interfaces are identified according to singularity in terms of interfacial defects: ledges and dislocations. The structure singularities are defined by the elimination of one or more classes of defects, which must be present in the vicinal interfaces. Four classes of interfaces have been classified, with a new class—CS-coherent—added to the common list of coherent, semicoherent, and incoherent. An interface with a CS-coherent structure is in a secondary preferred state, in contrast to a coherent or semicoherent in the primary preferred state. All four classes of interfaces can be singular according to singularity in the ledge structure. Such a singular interface is normal to a low index $\mathbf{g}_{\text{P-I}}$ vector from both or either crystal across the interface. Singular interfaces are probably more often influenced by singularity in the dislocation structure. Only coherent, semicoherent and CS-coherent can be singular according to singularity in the dislocation structure. The preferred state in the areas between the dislocations must be specified in a calculation of the dislocation structure.

The O-lattice theory has been applied to specify the geometry of the singular interfaces that exhibit singularity in terms of dislocation defects. The basic concepts and major formulas of the O-lattice theory are reviewed mainly for the interfaces in the primary preferred state. The selection of $\mathbf{A}$ matrix is intentionally discussed to clarify ambiguity about its selection in the literature. The advantages of the O-lattice approach over the Frank–Bilby equation for the calculation of dislocation structure are highlighted. It is found from the O-lattice analysis that all principal O-lattice planes are candidates of singular interfaces with respect to any deviation in IO. Based on the association between the principal O-lattice planes and $\Delta\mathbf{g}_{\text{P-I}}$s, it is concluded that a singular coherent or semicoherent interface is always normal to at least one $\Delta\mathbf{g}_{\text{P-I}}$, associated with a low index $\mathbf{g}_{\text{P-}\alpha}$ and $\mathbf{g}_{\text{P-}\beta}$. In general, an interface normal to any one $\Delta\mathbf{g}_{\text{P-I}}$ is a candidate for interfaces that is singular fully with respect to the IO. The results of the O-lattice study have been extended to analyze interfaces in secondary preferred states. Any singular CS-coherent interface is parallel to a principal secondary O-lattice plane that is normal to a $\Delta\mathbf{g}_{\text{P-II}}$. Since a secondary preferred state is confined in a plane, the specific ledges with terraces parallel to this plane are treated as "physical" dislocations in the singularity analysis, even though they are not so calculated in the secondary O-lattice calculation.

An interface that is singular with respect to the OR contains a structure of reduced defects, which is possible at a special OR. The role of ledges is integrated into the conditions for optimizing the OR. The OR corresponding to a singular interface can be described by one or more of the three $\Delta\mathbf{g}$ parallelism rules. Each $\Delta\mathbf{g}$ parallelism rule constrains four degrees of freedom in the macroscopic geometry of a singular interface, but one degree of freedom in the OR is unfixed. Further reduction of defects, such as in a coherent interface, is possible only when the lattice parameters are special to permit the system to obey two $\Delta\mathbf{g}$ parallelism rules. The corresponding singular interface is then fully fixed. Usually a supplementary constraint is

adopted by a system, and the geometry of a singular interface is thus fixed. Therefore, a singular interface normal to a group of reciprocal vectors including at least one $\Delta\mathbf{g}$ is singular fully respect to the IO and it is also singular fully or partially respect to the OR.

The present approach provides limited number of candidates of singular interfaces, but it usually cannot predict a unique point in the 5D BGP space for the OR and IO of a singular interface to be observed. These candidates can greatly reduce the calculation work required for a physical model to determine the minimum interfacial energy in the 5D space. Identification of singular interfaces using $\Delta\mathbf{g}$s is experimentally convenient, because these reciprocal vectors and their associated Moiré fringes are measurable with TEM. The identities and roles of different defects are discussed. A discussion was also made to clarify the limitations of the approach and to suggest further study.

Acknowledgements Financial support from National Nature Science Foundation of China (No. 50971076) and National Basic Research Program of China (No. 2009CB623704) from Chinese Ministry of Science and Technology are gratefully acknowledged. The Authors wish to thank Professors A.P. Sutton and R.C. Pond for valuable discussions during iib 2010, to Mr. X.-F. Gu and Mr. Z.-Z. Shi for kind assistance in preparation of the manuscript, and to Mr. C. Ocier and Ms. S. Hadian for helpful proof reading, and to the reviewers for kind helps in providing many useful corrections and suggestions especially in English writing.

References

1. Howe JM (1997) Interfaces in materials. Wiley, New York
2. Sutton AP, Balluffi RW (1995) Interfaces in crystalline materials. Oxford University Press, Oxford
3. Erwin SC, Zu L, Haftel MI, Efros AL, Kennedy TA, Norris DJ (2005) Nat Lett 436(7):91
4. Moll N, Kley A, Pehlke E, Scheffler M (1996) Phy Rev B 54(12):8844
5. Che JG, Chan CT (1998) Phys Rev B 57(3):1875
6. Zhang W-Z, Weatherly GC (2005) Prog Mater Sci 50(2):181
7. Zhang M-X, Kelly PM (2009) Prog Mater Sci 54:1101
8. Bollmann W, Nissen H-U (1968) Acta Cryst 24A(5):546
9. Bollmann W (1970) Crystal defects and crystalline interfaces. Springer, Berlin
10. Zhang W-Z, Shi Z-Z (2011) Solid State Phenom (in press)
11. Bollmann W (1982) Crystal lattices, interfaces, matrices. Bollmann, Geneva
12. Zhang W-Z, Purdy GR (1993) Philos Mag 68A(2):291
13. Zhang W-Z, Purdy GR (1993) Philos Mag 68A(2):279
14. Tiller WA (1991) The science of crystallization: microscopic interfacial phenomena. Cambridge University Press, New York
15. Ye F, Zhang WZ (2002) Acta Mater 50(11):2761
16. Zhang M, Zhang W-Z, Ye F (2005) Metall Mater Trans 36A (7):1681
17. Christian JW (2002) The theory of transformation in metals and alloys, 3rd edn. Pergamon Press, Oxford, UK
18. Porter DA, Easterling KE (1992) Phase transformations in metals and alloys. Chapman and Hall, New York
19. Frank FC (1950) In: Symposium on the plastic deformation of crystalline solids, pp 150
20. Bilby BA (1955) In: Report on the conference on defects in crystalline solids, The Physical Society, London, pp 124
21. Wayman CM (1964) Introduction to the crystallography of martensitic transformations. MacMillan, New York
22. Bollmann W (1974) Phys Stat Solid A21:543
23. Zhang W-Z (2005) Appl Phys Lett 86(12):121919
24. Hirth JP, Lothe J (1992) Theory of dislocations, 2nd edn. Krieger Publishing Company, Malabar, FL
25. Qiu D, Zhang W-Z (2008) Acta Mater 56:2003
26. Zhang W-Z (1998) Philos Mag 78(4):913
27. Pitsch W (1959) Philos Mag 4(41):577
28. Hirsch P, Howe A, Nicholson R, Pashley DW, Whelan MJ (1977) Electron microscopy of thin crystals, 2nd edn. Robert E. Krieger Publishing Company, Malabar, FL
29. Duly D, Zhang WZ, Audier M (1995) Philos Mag 71A(1):187
30. Khachaturyan AG (1983) Theory of structural transformations in solids. Wiley, New York
31. Ye F, Zhang W-Z, Qiu D (2006) Acta Mater 54:5377
32. Zhang W-Z, Qiu D, Yang XP, Ye F (2006) Metall Mater Trans A 37:911
33. Gu X-F, Zhang W-Z (2010) Philos Mag 90:4503
34. Hall MG, Aaronson HI, Kinsma KR (1972) Surf Sci 31:257
35. Wu J, Zhang W-Z, Gu X-F (2009) Acta Mater 57:635
36. Gu X-F, Zhang W-Z (2010) Philos Mag 90:3281
37. Xiao SQ, Howe JM (2000) Acta Mater 48(12):3253
38. Kelly PM, Zhang MX (1999) Mater Forum 23:41
39. Zhang W-Z (1997) Scripta Mater 37(2):187
40. Grimmer H (1974) Scripta Metall 8(11):1221
41. Zhang W-Z, Ye F, Zhang C, Qi Y, Fang HS (2000) Acta Mater 48(9):2209
42. Hirth JP, Pond RC (1996) Acta Mater 44(12):4749
43. Pond R, Ma X, Chai Y, Hirth J (2007) In: Nabarro FRN, Hirth JP (eds) Dislocations in solids, vol 13. Elsevier, Amsterdam
44. Olson GB, Cohen M (1979) Acta Metall 27(12):1907
45. Babcock SE, Balluffi RW (1987) Philos Mag 55:643